scribe the systematic modification of the aromatic ring of **3** for further optimization to evaluate substituent effects on anti-HIV activity, cytotoxicity and CD4 mimicry.

2. Results and discussion

The co-crystal structure of **1** with the gp120 core revealed that the aromatic group of **1** binds to gp120 by several aromatic–aromatic and hydrophobic interactions (Fig. 2). In particular, hydrophobic space surrounded by the hydrophobic amino acid residues Trp112, Val255, Phe382, and Ile424 is likely to be affected by substituents at the *meta*- and *para*-positions of the aromatic ring, and consequently we decided to investigate substituents at these positions (Fig. 3).

Initially, we selected a chlorine or a methyl group to serve as the *para*-substituent of the aromatic group because CD4 mimic compounds such as **1** (NBD-556) with a *p*-chloro substituent, and because **3** showed significant anti-HIV activity compared to other substituents. Further, CD4 mimic structures such as **2** with a *p*-methyl substituent also showed potent anti-HIV activity and exhibits lower cytotoxicity than those with the *p*-chlorophenyl derivatives.[8a] Next, we chose several halogens including F, Cl and Br, to be the *meta*-substituent on the aromatic group since previous SAR studies revealed that the introduction of an appropriate group with an electron-withdrawing ability at the *meta*-position leads to an increase of binding affinity and antiviral activity.[6a] Furthermore, to investigate whether electron withdrawal and hydrophobicity of the *meta*-position are appropriate, the CD4 mimics with a *meta*-methyl substituent, which has electron-donating properties and is similar in size to bromine, were also synthesized. Finally, two piperidine scaffolds (the 2,2,6,6-tetramethylpiperidine **A** and the dicyclohexylpiperidine **B**) were combined with these aromatics via the oxalamide linker.

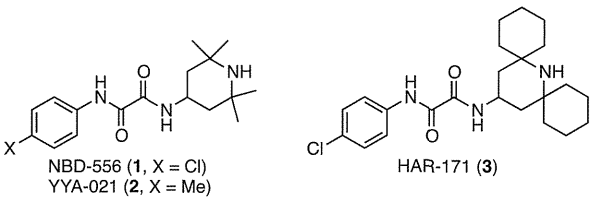

Figure 1. Structures of NBD-556 (**1**), YYA-021 (**2**) and HAR-171 (**3**).

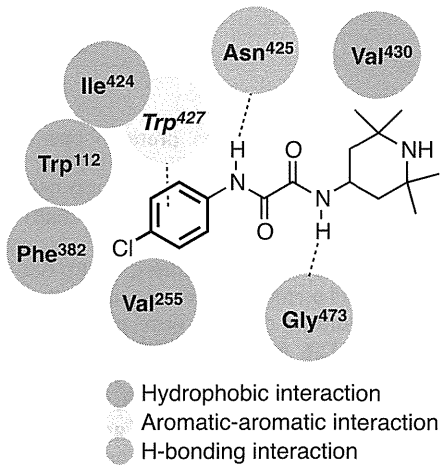

Figure 2. Major interactions between NBD-556 and Phe43 cavity of gp120.

2.1. Chemistry

The syntheses of novel compounds are depicted in Schemes 1 and 2. Starting from the appropriate aniline with *m*- and *p*-substituents, coupling with ethyl chloroglyoxylate in the presence of Et_3N gave the corresponding amidoesters **6a–c** and **7a–c**. Subsequently, microwave-assisted aminolysis[13] of **6a–c** and **7a–c** with commercially available 4-amino-2,2,6,6-tetramethylpiperidines afforded the desired compounds **8a–c** and **9a–c** (Scheme 1). A series of CD4 mimics with two cyclohexyl groups **13a–c** and **14a–c** were prepared from 2,2,6,6-tetramethylpiperidin-4-one **10** by the method previously reported,[8c] with slight modification (Scheme 2). Briefly, treatment of **10** with cyclohexanone in the presence of ammonium chloride gave a 2,6-substituted piperidin-4-one **11** via Grob fragmentation followed by intramolecular cyclization.[14] Reductive amination with *p*-methoxybenzyl amine, acidic treatment with TMSBr/TFA, and oxidative cleavage of *p*-methoxybenzyl group with cerium(IV) ammonium nitrates (CAN) furnished the corresponding 4-aminopiperidines (**12**) with higher yields and less burdensome purifications than the previous method. Finally, coupling of **12** with the corresponding esters **6a–c** and **7a–c** under microwave irradiation provided the desired compounds **13a–c** and **14a–c**.

2.2. Biological evaluation

The anti-HIV activity of the synthetic compounds was evaluated against an R5 primary isolate YTA strain. IC_{50} values were determined by the WST-8 method as the concentrations of the compounds that conferred 50% protection against HIV-1-induced cytopathogenicity in PM1/CCR5 cells. Cytotoxicity of the compounds based on the viability of mock-infected PM1/CCR5 cells was also evaluated using the WST-8 method. The assay results for compounds **8a–c** and **13a–c** with a *p*-chlorophenyl group are shown in Table 1. The parent compound **1** and compound **8a**,[6a] known as JRC-II-191, showed significant anti-HIV activities (IC_{50}

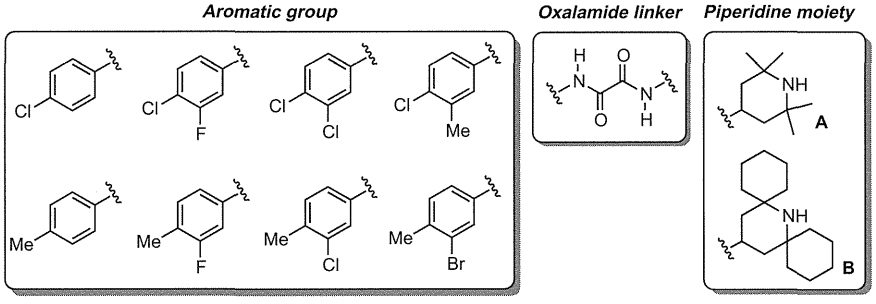

Figure 3. The structures of scaffolds in the design of novel CD4 mimics.

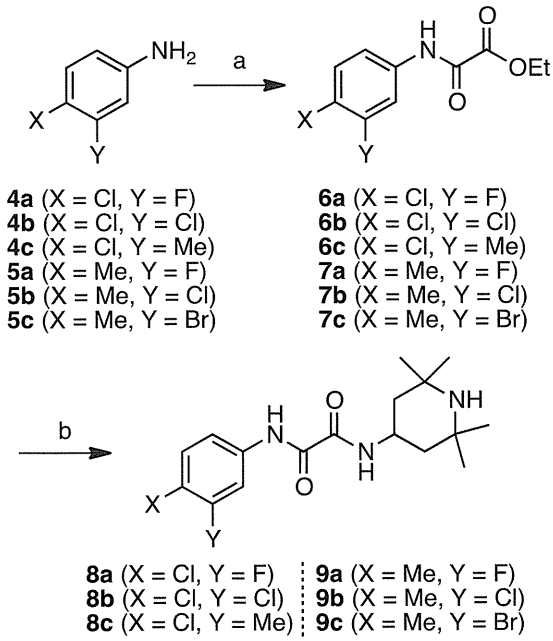

Scheme 1. Reagents and conditions: (a) ethyl chloroglyoxylate, Et_3N, THF; (b) 4-amino-2,2,6,6-tetramethylpiperidine, Et_3N, EtOH, 150 °C, microwave.

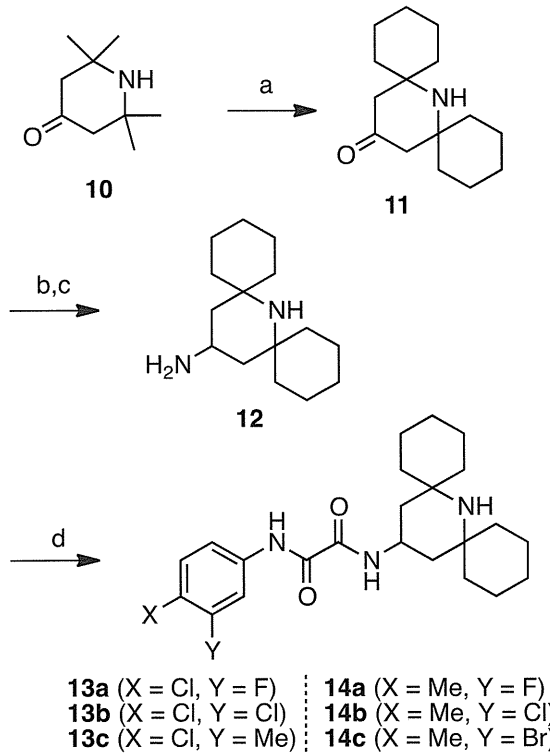

Scheme 2. Reagents and conditions: (a) cyclohexanone, NH_4Cl, DMSO, 60 °C; (b) *p*-methoxybenzylamine, $NaBH_3CN$, MeOH, then 1 M TMSBr in TFA; (c) CAN, CH_3CN/H_2O (v:v = 2:1); (d) **6** or **7**, Et_3N, EtOH, 150 °C, microwave.

of **1** = 0.61 μM and IC_{50} of **8a** = 0.32 μM). Compound **8b**[6a] having a *m,p*-dichlorophenyl group and compound **8c**[6a] (JRC-II-193) having a *p*-chloro-*m*-tolyl group showed moderate anti-HIV activity (IC_{50} of **8b** = 4.1 μM and IC_{50} of **8c** = 3.3 μM) but their potency was

Table 1
Anti-HIV activity and cytotoxicity of compounds **8a–c** and **13a–c** containing a *p*-chlorophenyl group[a]

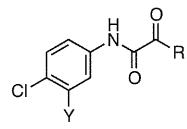

Compd	R	Y	IC_{50}[b] (μM) YTA48P	CC_{50}[c] (μM)
1	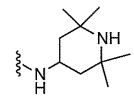	H	0.61	110
8a	**A**	F	0.32	94
8b	**A**	Cl	4.1	36
8c	**A**	Me	3.3	38
3	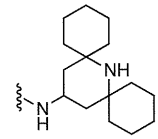	H	0.43	120
13a	**B**	F	0.23	11
13b	**B**	Cl	0.62	11
13c	**B**	Me	2.6	15

[a] All data are the mean values from three of more independent experiments.
[b] IC_{50} values of the multi-round assay are based on the inhibition of HIV-1-induced cytopathogenicity in PM1/CCR5 cells.
[c] CC_{50} values are based on the reduction of the viability of mock-infected PM1/CCR5 cells.

Table 2
Anti-HIV activity and cytotoxicity of compounds **9a–c** and **14a–c** containing a *p*-tolyl group[a]

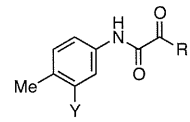

Compd	R	Y	IC_{50}[b] (μM) YTA48P	CC_{50}[c] (μM)
2	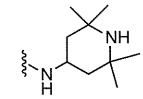	H	9.0	260
9a	**A**	F	2.8	110
9b	**A**	Cl	3.2	62
9c	**A**	Br	>10	32
14a	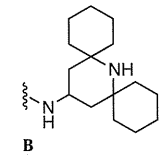	F	0.54	91
14b	**B**	Cl	6.2	11
14c	**B**	Br	3.2	11

[a] All data are the mean values from three of more independent experiments.
[b] IC_{50} values of the multi-round assay are based on the inhibition of HIV-1-induced cytopathogenicity in PM1/CCR5 cells.
[c] CC_{50} values are based on the reduction of the viability of mock-infected PM1/CCR5 cells.

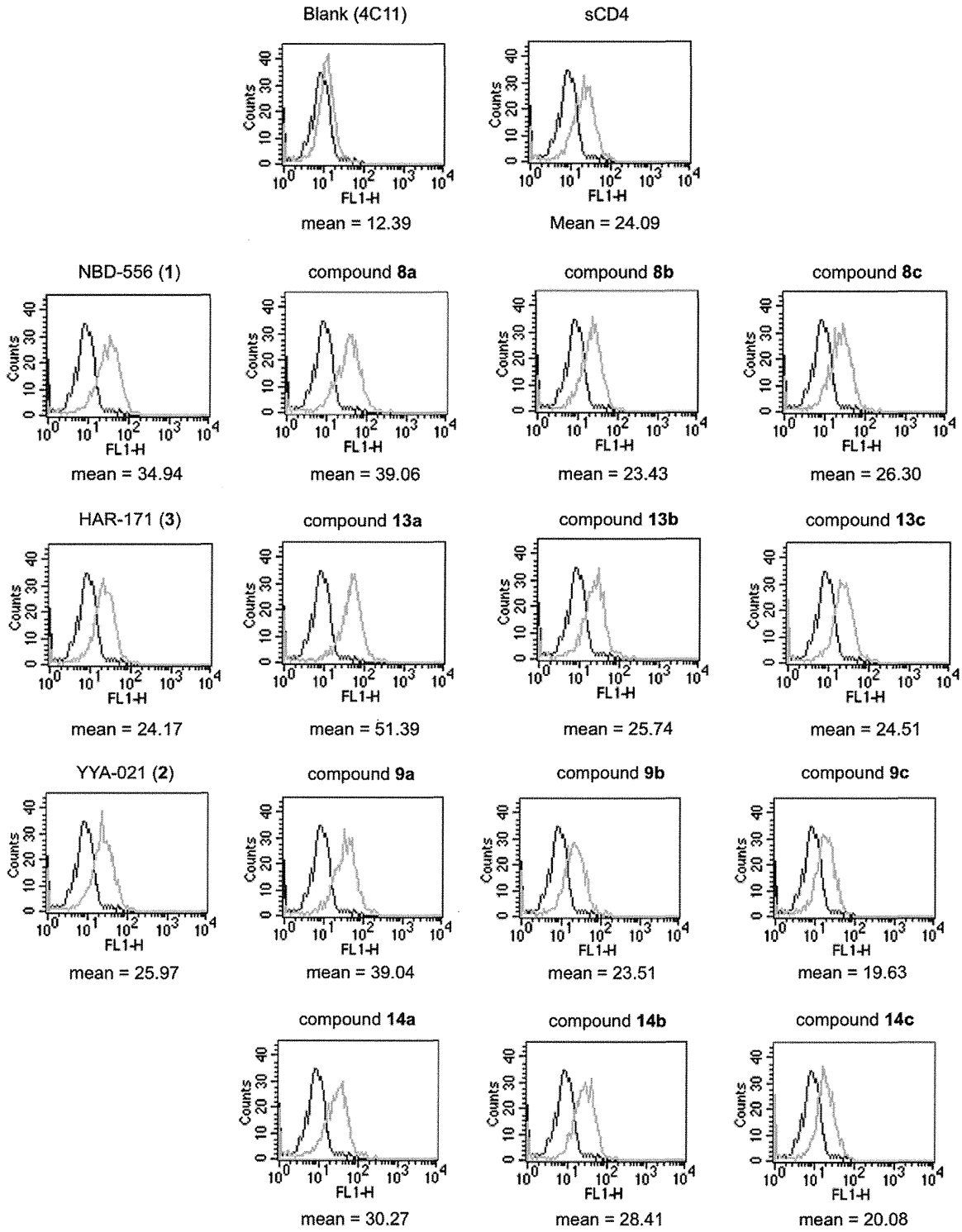

Figure 4. FACS analysis of synthetic compounds **8**, **9**, **13** and **14**.

approximately 10-fold lower than that of compound **8a**. The cytotoxicity of **8b** and **8c** is relatively stronger than that of **8a** (CC_{50} of **8b** = 36 μM and CC_{50} of **8c** = 38 μM). Compounds **13a–c** with hydrophobic cyclohexyl groups in the piperidine moiety showed more potent anti-HIV activity than the corresponding compounds **8a–c**, confirming the contribution of the bulky hydrophobic group(s) to an increase of antiviral activity. Our lead compound **3** showed significant anti-HIV activity comparable to that of compound **8a** (IC_{50} = 0.43 μM) but, consistent with previous results, exhibited lower cytotoxicity. In particular, compound **13a** with a *m*-fluoro-*p*-chlorophenyl group exhibited the highest anti-HIV activity. The IC_{50} value of **13a** was 0.23 μM, whose potency was

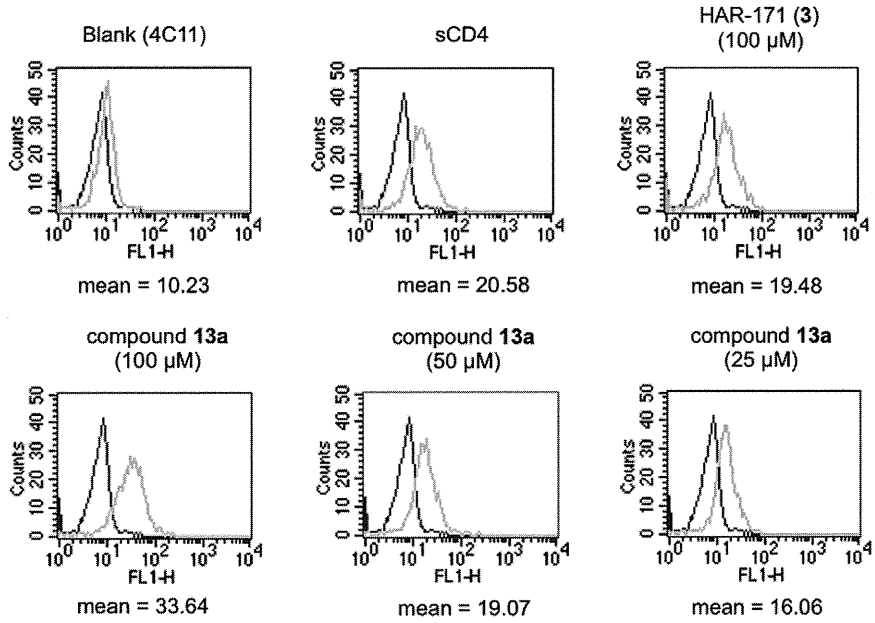

Figure 5. FACS analysis of **3** and **13a** in different concentrations.

approximately twice as high as that of compound **3**. Notably, compound **13b** with a *m,p*-dichlorophenyl group showed 7-fold more potent anti-HIV activity than the corresponding compound **8b**. Compound **13c**, which has a *p*-chloro-*m*-tolyl group, showed potent anti-HIV activity comparable to that of the corresponding compound **8c** and an increase of cytotoxicity (CC_{50} = 15 μM). We observed a tendency for compounds **13a–c** with both hydrophobic cyclohexyl groups and a *m,p*-disubstituted phenyl group to exhibit higher cytotoxicity than the corresponding tetramethyl-type compounds **8a–c**. No clear reason for an increase of cytotoxicity in the *m,p*-disubstituted phenyl group-containing compounds is apparent.

Assay results for the compounds **9a–c** and **14a–c** with a *p*-tolyl group are shown in Table 2. As expected, replacement of the *p*-chloro substituent with a *p*-methyl group resulted in somewhat reduction of anti-HIV activity. Compound **2**, YYA-021 has significant anti-HIV activity (IC_{50} = 9.0 μM) and exhibits the lowest cytotoxicity among all of the compounds tested (CC_{50} = 260 μM). These results are consistent with our previous SAR studies involving the aromatic ring. Introduction of a fluorine at the *meta*-position of the *p*-tolyl group, e.g. in compound **9a** and **14a**, improved the antiviral activity, as observed with **8a** and **13a** and a similar tendency was observed for compound **9b** with a *m*-chloro-*p*-tolyl group. In particular, compound **14a** with cyclohexyl groups and a *m*-fluoro-*p*-tolyl group showed slightly higher anti-HIV activity than the parent compound **1**. Among the compounds with *m*-bromo-*p*-tolyl groups, it was found that compound **9c**, with a 2,2,6,6-tetramethylpiperidine group, showed no anti-HIV activity at a concentration below 10 μM, whereas compound **14c** with hydrophobic cyclohexyl groups attached to the piperidine moiety, showed moderate activity (IC_{50} = 3.2 μM), indicating that the hydrophobic modification of piperidine ring can contribute to an increase in anti-HIV activity.

All the synthetic compounds were evaluated for their CD4 mimicry on the conformational changes in gp120 by fluorescence activated cell sorting (FACS) analysis, and the results are shown in Figure 4. The profile of binding of a CD4-induced (CD4i) monoclonal antibody (4C11) to the Env-expressing cell surface pretreated with the synthetic compounds was assessed in terms of the mean fluorescence intensity (MFI). The increase in binding affinity for 4C11 (by the pretreatment with synthetic compounds) suggests that those compounds can reflect the CD4 mimicry as a consequence of the conformational changes in gp120. Our previous studies disclosed that the profiles of the binding to the cell surface pretreated with **1**, **2**, or **3** were similar to those observed in pretreatment with soluble CD4, indicating that these compounds offer a significant enhancement of binding affinity for 4C11.[8] As shown in Figure 4, similar results were obtained with those compounds in this FACS analysis (MFI of **1**, **2**, and **3** = 34.94, 25.97, and 24.17, respectively). A notable increase in binding affinity for 4C11 was observed in essentially all the synthetic compounds. The compounds **8a**, **9a**, **13a** and **14a** with a *meta*-fluorine in the aromatic ring, showed significant anti-HIV activity, and produced a substantial increase in binding affinity for 4C11. These results suggested that the introduction of a fluorine group at the meta position of the aromatic ring is significant not only for the increase of anti-HIV activity, but also for the enhancement of a CD4 mimicry. In particular, a remarkable improvement in binding affinity for 4C11 was observed with **13a** (MFI = 51.39) which has twofold more potent anti-HIV activity than the lead compound **3** (HAR-171), and is the most active compound in terms of both anti-HIV activity and the CD4 mimicry resulting from the conformational change in gp120. The profiles of pretreatment of the cell surface with compounds **8b** and **13b** having a *m,p*-dichlorophenyl group, compounds **8c** and **13c** having a *p*-chloro-*m*-tolyl group, and compounds **9b** and **14b** with a *m*-chloro-*p*-tolyl group were similar to results obtained for **3**, suggesting that these compounds produced slightly lower enhancement compared to those of compounds **8a**, **9a**, **13a** and **14a** but significant levels of binding affinity for 4C11. On the other hand, pretreatment with compounds **9c**, which failed to show significant anti-HIV activity and **14c**, which had moderate anti-HIV activity resulted in a slight decrease of binding affinity for 4C11, suggesting that the introduction of a Br group at the *meta*-position of *p*-tolyl group is not advantageous to a CD4 mimicry, possibly due to the steric hindrance caused by the two bulky substituents. These results are consistent with previous observations that a limited size and electron-withdrawing ability of the aromatic substituents are required for potent anti-HIV activity and CD4 mimicry.[8a]

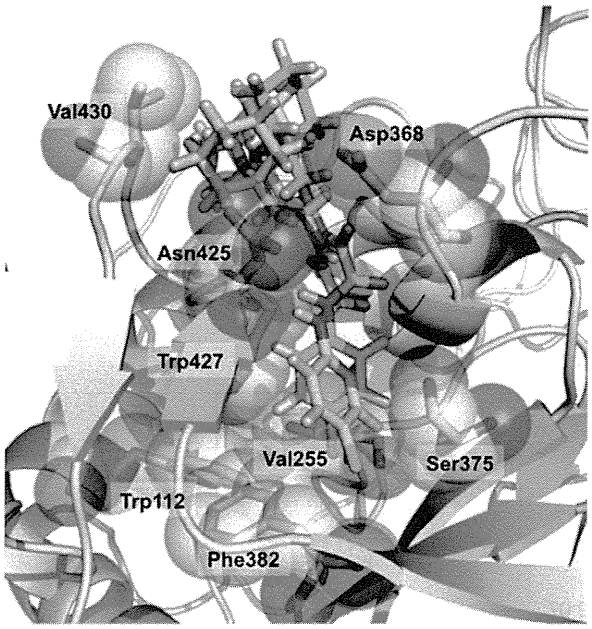

Figure 6. The modeled structure of **13a** (yellow carbon atoms) in the complex with the Phe43 cavity in gp120 (3TGS) overlaid with the modeled structure of **3** (green carbon atoms).

Since **13a** showed higher CD4 mimicry than the other compounds tested, the effect of the solution concentration of **13a** on the binding affinity for 4C11 was investigated. As shown in Figure 5, pretreatment of the cell surface with a 100 μM solution of **13a** produced a higher increase in the binding affinity for 4C11 than pretreatment with the same concentration of compound **3**. Interestingly, the profile pretreated with a 50 μM solution of **13a** was similar to that with a 100 μM of compound **3**, and even with a 25 μM solution of **13a** a potent enhancement of the binding affinity for 4C11 was observed: MFI of **13a** at concentrations of 50 μM and 25 μM = 19.07 and 16.06, respectively. This observation suggests that **13a** could serve as a novel lead compound for the development of envelope protein openers for the use combined with neutralizing antibodies because of its effectiveness at low concentrations.

The substantial increase in the CD4 mimicry of **13a** even at a low concentration is not easily explained because HAR-171 (**3**) and **13a** would be expected to form the similar binding modes with gp120. A probable contribution of **13a** is suggested by modeling studies docked into the Phe43 cavity in gp120 (3TGS) in which the depth and direction of the aromatic ring of **13a** is slightly different from those in compound **3** (Fig. 6), leading to the possible formation of appropriate interactions with the hydrophobic amino acid residues such as Val255 and Phe382, and therefore explaining the increased potency observed in the anti-HIV activity and CD4 mimicry of **13a**.

3. Conclusion

CD4 mimics are attractive agents not only for the development of a novel class of HIV entry inhibitors but also as possible cooperating agents for the neutralizing antibodies—that is, envelope protein openers. In the present study, a structure–activity relationship study of a series of CD4 mimic compounds was performed with a view to improving the biological activity of HAR-171 (**3**), which was identified in our previous studies as a promising lead compound with anti-HIV activity, cytotoxicity and CD4 mimicry resulting from the conformational change in gp120. Systematic modification of the *meta*- and *para*-substituents of the aromatic ring of **3** led to some potent compounds. In particular, **13a**, which has a bulky hydrophobic group on its piperidine ring and a *m*-fluoro-*p*-chlorophenyl group, demonstrated twofold more potent anti-HIV activity and much higher CD4 mimicry than **2** following the conformational changes in gp120, although the cytotoxicity of **13a** is relatively high. Further structural modification studies of the aromatic ring and the oxalamide linker to improve pharmaceutical profiles will be the subject of future reports.

4. Experimentals

^{1}H NMR and ^{13}C NMR spectra were recorded using a Bruker Avance III spectrometer. Chemical shifts are reported in δ (ppm) relative to Me_4Si (in $CDCl_3$) as internal standard. Low- and high-resolution mass spectra were recorded on a Bruker Daltonics microTOF focus in the positive and negative detection mode. For flash chromatography, silica gel 60 N (Kanto Chemical Co., Inc.) was employed. Microwave reactions were performed in Biotage Microwave Reaction Kit (sealed vials) in an Initiator™ (Biotage). The wattage was automatically adjusted to maintain the desired temperature for the desired period of time.

4.1. Chemistry

4.1.1. Ethyl 2-((4-chloro-3-fluorophenyl)amino)-2-oxoacetate (6a)

To a stirred solution of 3-fluoroaniline (1.11 g, 10.0 mmol) in $CHCl_3$ (30.0 mL) was added dropwise *N*-chlorosuccinimide (NCS) in $CHCl_3$ (20.0 mL) at 0 °C. The mixture was stirred at 0 °C for 42 h. After the reaction mixture was concentrated under reduced pressure, the residue was dissolved in Et_2O. The mixture was washed with water, and dried over $MgSO_4$. Concentration under reduced pressure followed by flash chromatography over silica gel with EtOAc/*n*-hexane gave 4-chloro-3-fluoroaniline (259.4 g, 18% yield) as crystalline solids. To a stirred solution of the above aniline (259.4 mg, 1.78 mmol) in THF (8.9 mL) were added at 0 °C ethyl chloroglyoxylate (237.3 μL, 2.14 mmol) and Et_3N (296.6 μL, 2.14 mmol). The mixture was stirred at room temperature for 12 h. After the precipitate was filtrated off, the filtrate solution was concentrated under reduced pressure. The residue was dissolved in EtOAc, and washed with 1.0 M HCl, saturated $NaHCO_3$ and brine, then dried over $MgSO_4$. Concentration under reduced pressure to provide the title compound **6a** (435.2 mg, 99% yield) as brown crystals, which was used without further purification.

^{1}H NMR (500 MHz, $CDCl_3$) δ 1.44 (t, J = 7.50 Hz, 3H), 4.43 (q, J = 7.50 Hz, 2H), 7.24–7.25 (m, 1H), 7.35–7.40 (m, 1H), 7.70–7.75 (m, 1H), 8.93 (br, 1H); ^{13}C NMR (125 MHz, $CDCl_3$) δ 13.0, 64.1, 108.5 (d, J = 26.3 Hz), 115.9 (d, J = 3.75 Hz), 117.3 (d, J = 18.8 Hz), 130.9 (d, J = 10.0 Hz), 135.9, 153.9, 158.1 (d, J = 246.3 Hz), 160.5; HRMS (ESI), *m*/*z* calcd for $C_{10}H_{10}ClFNO_3$ (MH^-) 244.0182, found 244.0183.

4.1.2. Ethyl 2-((3,4-dichlorophenyl)amino)-2-oxoacetate (6b)

To a stirred solution of 3,4-dichloroaniline **4b** (1.94 g, 12.0 mmol) in THF (20.0 mL) were added ethyl chloroglyoxylate (1.11 mL, 10.0 mmol) and Et_3N (15.2 mL, 11.0 mmol) at 0 °C. The mixture was stirred at room temperature for 6 h. After the precipitate was filtrated off, the filtrate solution was concentrated under reduced pressure. The residue was dissolved in EtOAc, and washed with 1.0 M HCl, saturated $NaHCO_3$ and brine, then dried over $MgSO_4$. Concentration under reduced pressure to provide the title compound **6b** (1.58 g, 95% yield) as white powder, which was used without further purification.

^{1}H NMR (500 MHz, $CDCl_3$) δ 1.44 (t, J = 7.00 Hz, 3H), 4.43 (q, J = 7.00 Hz, 2H), 7.44 (d, J = 8.50 Hz, 1H), 7.49–7.51 (m, 1H), 7.87, 2.35 (d, J = 2.50 Hz, 1H); ^{13}C NMR (125 MHz, $CDCl_3$) δ 14.0, 64.0, 119.0, 121.5, 129.0, 130.8, 133.2, 135.7, 153.9, 160.5; HRMS (ESI), m/z calcd for $C_{10}H_{10}Cl_2NO_3$ (MH^+) 262.0038, found 262.0031.

4.1.3. Ethyl 2-((4-chloro-3-methylphenyl)amino)-2-oxoacetate (6c)

By use of a procedure similar to that described for the preparation of compound **6b**, the aniline **4c** (3.34 g, 24.0 mmol) was converted into the title compound **6c** (4.63 g, 96% yield) as white powder.

^{1}H NMR (500 MHz, $CDCl_3$) δ 1.43 (t, J = 7.00 Hz, 3H), 2.38 (s, 3H), 4.42 (q, J = 7.00 Hz, 2H), 7.33 (d, J = 8.50 Hz, 1H), 7.43–7.46 (m, 1H), 7.51–7.54 (m, 1H), 8.82 (s, 1H); ^{13}C NMR (125 MHz, $CDCl_3$) δ 14.0, 20.2, 63.8, 118.5, 122.0, 129.7, 130.9, 134.8, 137.1, 153.8, 160.9; HRMS (ESI), m/z calcd for $C_{11}H_{13}ClNO_3$ (MH^+) 242.0578, found 242.0568.

4.1.4. Ethyl 2-((3-fluoro-4-methylphenyl)amino)-2-oxoacetate (7a)

By use of a procedure similar to that described for the preparation of compound **6b**, the aniline **5a** (3.00 g, 24.0 mmol) was converted into the title compound **7a** (4.24 g, 94% yield) as white powder.

^{1}H NMR (500 MHz, $CDCl_3$) δ 1.43 (t, J = 7.20 Hz, 3H), 2.25 (s, 3H), 4.42 (q, J = 6.80 Hz, 2H), 7.12–7.21 (m, 2H), 7.48–7.56 (m, 1H), 8.83 (s, 1H); ^{13}C NMR (125 MHz, $CDCl_3$) δ 14.2 (2C), 63.8, 107.1 (d, J = 27.5 Hz), 115.0 (d, J = 10.0 Hz), 122.3 (d, J = 17.5 Hz), 131.6 (d, J = 6.25 Hz), 135.3 (d, J = 13.8 Hz), 153.8, 160.8, 161.1 (d, J = 243.8 Hz); HRMS (ESI), m/z calcd for $C_{11}H_{13}FNO_3$ (MH^+) 226.0879, found 226.0878.

4.1.5. Ethyl 2-((3-chloro-4-methylphenyl)amino)-2-oxoacetate (7b)

By use of a procedure similar to that described for the preparation of compound **6b**, the aniline **5b** (3.40 g, 24.0 mmol) was converted into the title compound **7b** (5.19 g, 94% yield) as white powder.

^{1}H NMR (500 MHz, $CDCl_3$) δ 1.43 (t, J = 7.00 Hz, 3H), 2.35 (s, 3H), 4.42 (q, J = 7.00 Hz, 2H), 7.22 (d, J = 8.50 Hz, 1H), 7.41–7.43 (m, 1H), 7.71 (d, J = 2.00 Hz, 1H), 8.83 (s, 1H); ^{13}C NMR (125 MHz, $CDCl_3$) δ 14.0, 20.0, 63.8, 118.0, 120.3, 131.2, 133.3, 134.7, 135.0, 153.8, 160.8; HRMS (ESI), m/z calcd for $C_{11}H_{13}ClNO_3$ (MH^+) 242.0584, found 242.0573.

4.1.6. Ethyl 2-((3-bromo-4-methylphenyl)amino)-2-oxoacetate (7c)

By use of a procedure similar to that described for the preparation of compound **6b**, the aniline **5c** (4.47 g, 27.0 mmol) was converted into the title compound **7c** (6.24 g, 96% yield) as white powder.

^{1}H NMR (500 MHz, $CDCl_3$) δ 1.43 (t, J = 7.00 Hz, 3H), 2.38 (s, 3H), 4.42 (q, J = 7.00 Hz, 2H), 7.23 (t, J = 8.50 Hz, 1H), 7.48–7.53 (m, 1H), 7.83–7.90 (m, 1H), 8.80 (s, 1H); ^{13}C NMR (125 MHz, $CDCl_3$) δ 14.0, 22.4, 63.9, 118.7, 123.4, 125.0, 131.0, 135.0, 135.2, 153.7, 160.8; HRMS (ESI), m/z calcd for $C_{11}H_{13}BrNO_3$ (MH^+) 286.0079, found 286.0068.

4.1.7. N^1-(4-Chloro-3-fluorophenyl)-N^2-(2,2,6,6-tetramethylpiperidin-4-yl)oxalamide (8a)

To a solution of compound **6a** (70.0 mg, 0.286) in EtOH (2.9 mL) were added Et_3N (0.200 mL, 1.45 mmol) and 2,2,6,6-tetramethylpiperidin-4-amine (0.150 mL, 0.870 mmol). The reaction mixture was stirred for 3 h at 150 °C under microwave irradiation. After being concentrated in vacuo, the residue was extracted with $CHCl_3$, and washed with saturated $NaHCO_3$ and brine, then dried over $MgSO_4$. Concentration under reduced pressure to provide the title compound **8a** (34.6 mg, 34% yield) as white powder.

^{1}H NMR (500 MHz, $CDCl_3$) δ 0.99–1.50 (m, 15H), 1.92 (dd, J = 3.50, 9.00 Hz, 2H), 4.20–4.32 (m, 1H), 7.21–7.25 (m, 1H), 7.34–7.41 (m, 1H), 7.69–7.73 (m 1H), 9.31 (br, 1H); ^{13}C NMR (125 MHz, $CDCl_3$) δ 28.4, 34.8, 43.8, 44.5, 51.0, 108.3 (d, J = 26.3 Hz), 115.8 (d, J = 3.75 Hz), 117.1 (d, J = 17.5 Hz), 130.8, 136.2 (d, J = 8.75 Hz), 157.6, 158.1 (d, J = 247.5 Hz), 158.4; HRMS (ESI), m/z calcd for $C_{17}H_{24}ClFN_3O_2$ (MH^+) 356.1536, found 356.1548.

4.1.8. N^1-(3,4-Dichlorophenyl)-N^2-(2,2,6,6-tetramethylpiperidin-4-yl)oxalamide (8b)

By use of a procedure similar to that described for the preparation of compound **8a**, the compound **6b** (261.0 mg, 1.00 mmol) was converted into the title compound **8b** (520.0 mg, 70% yield) as white powder.

^{1}H NMR (500 MHz, $CDCl_3$) δ 1.07 (t, J = 12.0 Hz, 2H), 1.16 (s, 6H), 1.28 (s, 6H), 1.90–1.93 (m, 2H), 4.20–4.32 (m, 1H), 7.26 (m, 1H), 7.40–7.48 (m, 2H), 7.88 (s, 1H), 9.33 (s, 1H); ^{13}C NMR (125 MHz, $CDCl_3$) δ 28.5 (2C), 34.9 (2C), 43.8, 44.6 (2C), 50.9 (2C), 119.0, 121.4, 128.7, 130.8, 133.1, 135.8, 157.7, 158.5; HRMS (ESI), m/z calcd for $C_{17}H_{22}Cl_2N_3O_2$ (MH^-) 370.1095, found 370.1105.

4.1.9. N^1-(4-Chloro-3-methylphenyl)-N^2-(2,2,6,6-tetramethylpiperidin-4-yl)oxalamide (8c)

By use of a procedure similar to that described for the preparation of compound **8a**, the compound **6c** (482.0 mg, 2.00 mmol) was converted into the title compound **8c** (364.0 mg, 49% yield) as white powder.

^{1}H NMR (500 MHz, $CDCl_3$) δ 1.07 (t, J = 12.0 Hz, 2H), 1.15 (s, 6H), 1.28 (s, 6H), 1.86–1.94 (m, 2H), 4.15–4.31 (m, 1H), 7.21–7.24 (m, 1H), 7.32–7.38 (m, 2H), 7.74 (s, 1H), 9.24 (s, 1H); ^{13}C NMR (125 MHz, $CDCl_3$) δ 19.6, 28.5 (2C), 34.9 (2C), 43.7, 44.7 (2C), 50.9 (2C), 117.9, 120.2, 131.2, 133.1, 134.7, 135.1, 157.5, 158.8; HRMS (ESI), m/z calcd for $C_{18}H_{25}ClN_3O_2$ (MH^-) 350.1641, found 350.1656.

4.1.10. N^1-(3-Fluoro-4-methylphenyl)-N^2-(2,2,6,6-tetramethylpiperidin-4-yl)oxalamide (9a)

By use of a procedure similar to that described for the preparation of compound **8a**, the compound **7a** (225.0 mg, 1.00 mmol) was converted into the title compound **9a** (161.0 mg, 48% yield) as white powder.

^{1}H NMR (500 MHz, $CDCl_3$) δ 1.07 (t, J = 12.5 Hz, 2H), 1.15 (s, 6H), 1.28 (s, 6H), 1.92 (dd, J = 12.5, 3.50 Hz, 2H), 2.26 (s, 3H), 4.12–4.32 (m, 1H), 7.12–7.20 (m, 2H), 7.30–7.37 (m, 1H), 7.48–7.54 (m, 1H), 9.27 (s, 1H); ^{13}C NMR (125 MHz, $CDCl_3$) δ 14.2, 28.5 (2C), 34.9 (2C), 43.7, 44.7 (2C), 50.9 (2C), 107.1 (d, J = 26.3 Hz), 115.0, 121.8 (d, J = 17.5 Hz) 131.6, 135.4, (d, J = 15.0 Hz), 157.5, 158.8, 161.1 (d, J = 242.5 Hz); HRMS (ESI), m/z calcd for $C_{18}H_{25}FN_3O_2$ (MH^-) 334.1936, found 334.1942.

4.1.11. N^1-(3-Chloro-4-methylphenyl)-N^2-(2,2,6,6-tetramethylpiperidin-4-yl)oxalamide (9b)

By use of a procedure similar to that described for the preparation of compound **8a**, the compound **7b** (482.0 mg, 1.00 mmol) was converted into the title compound **9b** (448.0 mg, 48% yield) as white powder.

^{1}H NMR (500 MHz, $CDCl_3$) δ 1.09 (t, J = 12.5 Hz, 3H), 1.18 (s, 6H), 1.30 (s, 6H), 1.93–1.95 (m, 2H), 2.41 (s, 3H), 4.20–4.34 (m, 1H), 7.30–7.37 (m, 2H), 7.44–7.46 (m, 1H), 7.53 (d, J = 2.50 Hz, 1H), 9.25 (s, 1H); ^{13}C NMR (125 MHz, $CDCl_3$) δ 20.3, 28.5 (2C), 34.9 (2C), 43.7, 44.7 (2C), 50.9 (2C), 118.5, 122.0, 130.0, 130.7, 134.8, 137.1, 157.5, 158.8; HRMS (ESI), m/z calcd for $C_{18}H_{25}ClN_3O_2$ (MH^-) 350.1641, found 350.1636.

4.1.12. N^1-(3-Bromo-4-methylphenyl)-N^2-(2,2,6,6-tetramethylpiperidin-4-yl)oxalamide (9c)

By use of a procedure similar to that described for the preparation of compound **8a**, the compound **7c** (285.0 mg, 1.00 mmol) was converted into the title compound **9c** (157.0 mg, 40% yield) as white powder.

^{1}H NMR (500 MHz, $CDCl_3$) δ 1.07 (t, J = 12.5 Hz, 3H), 1.15 (s, 6H), 1.28 (s, 6H), 1.91 (dd, J = 8.00, 4.00 Hz, 2H), 2.38 (s, 3H), 3.70–3.75 (m, 1H), 7.22 (d, J = 8.50 Hz, 1H), 7.30–7.37 (m, 1H), 7.43–7.45 (m, 1H), 7.90 (d, J = 2.50 Hz, 1H), 9.25 (s, 1H); ^{13}C NMR (125 MHz, $CDCl_3$) δ 22.4, 28.5 (2C), 34.9 (2C), 43.7, 44.7 (2C), 50.9 (2C), 118.6, 123.4, 125.0, 131.0, 134.9 (2C), 157.5, 158.8; HRMS (ESI), m/z calcd for $C_{18}H_{25}BrN_3O_2$ (MH^-) 394.1136, found 394.1158.

4.1.13. Amine (12)

The compound **11** was prepared according to the reported procedure.[14] To a stirred solution of piridone **11** (247.8 mg, 1.05 mmol) in MeOH (2.10 mL) was added *p*-methoxybenzylamine (0.41 mL, 3.15 mmol). After being stirred at room temperature for 23 h, sodium cyanoborohydride was added and stirred at room temperature for 48 h. The reaction mixture was poured into saturated $NaHCO_3$ and extracted with EtOAc, then dried over $MgSO_4$. After concentration under reduced pressure, the residue was treated with 1 M TMS in THF (4.8 mL). The mixture was stirred at 0 °C for 14 h. Concentration under reduced pressure followed by short chromatography with $CHCl_3$/MeOH gave the PMB-protected amine. To a solution of the above amine (584.0 mg, 1.64 mmol) in CH_3CN/H_2O (13.1 mL, v:v = 2:1) was added CAN (2.74 g, 8.2 mmol). The mixture was stirred at room temperature for 14 h. The reaction mixture was diluted with 0.5 M HCl and washed with CH_2Cl_2. The water layer was alkalized and extracted with EtOAc, then dried over Na_2SO_4. Concentration under reduced pressure followed by flash chromatography over silica gel with EtOAc–EtOH (4:1) to gave the title compound **12** (175.5 mg, 71% yield) as a yellow oil.

^{1}H NMR (500 MHz, $CDCl_3$) δ 1.15–1.85 (m, 24H), 2.95–3.05 (m, 1H); ^{13}C NMR (125 MHz, $CDCl_3$) δ 22.2 (2C), 22.8 (2C), 26.2 (2C), 37.3 (2C), 42.3 (2C), 43.6 (2C), 47.0, 53.2 (2C); HRMS (ESI), m/z calcd for $C_{15}H_{29}N_2$ (MH^+) 237.2325, found 237.2321.

4.1.14. N^1-((4-Chloro-3-fluorophenyl)-N^2-(2,6-dicyclohexylpiperidin-4-yl)oxalamide (13a)

By use of a procedure similar to that described for the preparation of compound **8a**, the compound **6a** (36.8 mg, 0.150 mmol) was converted into the title compound **13a** (7.6 mg, 12% yield) as yellow powder.

^{1}H NMR (400 MHz, $CDCl_3$) δ 0.71–2.28 (m, 24H), 2.03–2.20 (m, 2H), 4.02–4.16 (m, 1H), 7.13–7.18 (m, 1H), 7.27–7.33 (m, 1H), 7.62–7.66 (m, 1H), 9.25 (br, 1H); ^{13}C NMR (125 MHz, $CDCl_3$) δ 14.1, 22.0 (2C), 22.6 (2C), 25.8 (2C), 29.3, 29.7 (2C), 31.9, 70.5, 108.3 (d, J = 26.3 Hz), 115.8, 117.1 (d, J = 18.8 Hz), 130.8, 136.2 (d, J = 10.0 Hz), 157.6, 158.1 (d, J = 247.5 Hz), 158.6; HRMS (ESI), m/z calcd for $C_{23}H_{32}ClFN_3O_2$ (MH^+) 436.2162, found 436.2156.

4.1.15. N^1-(4-Chlorophenyl)-N^2-(2,6-dicyclohexylpiperidin-4-yl)oxalamide (13b)

By use of a procedure similar to that described for the preparation of compound **8a**, the compound **6b** (31.3 mg, 0.120 mmol) was converted into the title compound **13b** (28.0 mg, 52% yield) as white powder.

^{1}H NMR (400 MHz, $CDCl_3$) δ 0.96 (t, J = 12.5 Hz, 2H), 1.10–1.84 (br, 20H), 2.05–2.19 (m, 2H), 4.08–4.21 (m, 1H), 7.23–7.33 (br, 1H), 7.39–7.46 (m, 2H), 7.88 (t, J = 1.00 Hz, 1H), 9.34 (s, 1H); ^{13}C NMR (125 MHz, $CDCl_3$) δ 14.1, 22.1 (2C), 22.7 (2C), 26.1 (2C), 31.6, 37.2 (2C), 42.6, 43.0, 43.6, 52.6 (2C), 119.0, 121.4, 128.7, 130.8, 133.1, 135.8, 157.7, 158.5; HRMS (ESI), m/z calcd for $C_{23}H_{32}Cl_2N_3O_2$ (MH^+) 452.1872, found 452.1865.

4.1.16. N^1-((4-Chloro-3-methylphenyl)-N^2-(2,6-dicyclohexylpiperidin-4-yl)oxalamide (13c)

By use of a procedure similar to that described for the preparation of compound **8a**, the compound **6c** (121.0 mg, 0.500 mmol) was converted into the title compound **13c** (15.1 mg, 7% yield) as white powder.

^{1}H NMR (500 MHz, $CDCl_3$) δ 0.87–1.88 (br, 22H), 2.09–2.20 (m, 2H), 2.38 (s, 3H), 4.09–4.22 (m, 1H), 7.32–7.33 (m, 1H), 7.41–7.43 (m, 1H), 7.51 (d, J = 2.00 Hz, 1H), 7.73 (m, 1H), 9.24 (s, 1H); ^{13}C NMR (125 MHz, $CDCl_3$) δ 20.2, 22.1 (2C), 22.7 (2C), 26.0 (2C), 29.7, 37.0, 42.3 (2C), 42.8 (2C), 43.4, 52.9 (2C), 118.4, 122.0, 130.0, 130.6, 134.8, 137.1, 157.5, 158.9; HRMS (ESI), m/z calcd for $C_{24}H_{35}ClN_3O_2$ (MH^+) 430.2267, found 430.2264.

4.1.17. N^1-(3-Fluoro-4-methylphenyl)-N^2-(2,6-dicyclohexylpiperidin-4-yl)oxalamide (14a)

By use of a procedure similar to that described for the preparation of compound **8a**, the compound **7a** (225.0 mg, 1.00 mmol) was converted into the title compound **14a** (27.5 mg, 7% yield) as white powder.

^{1}H NMR (500 MHz, $CDCl_3$) δ 0.971 (t, J = 12.5 Hz, 2H), 1.18–1.86 (m, 20H), 2.13–2.16 (m, 2H), 2.26 (s, 3H), 4.09–4.21 (m, 1H), 7.13–7.18 (m, 2H), 7.33 (d, J = 8.00 Hz, 1H), 7.50–7.53 (m, 1H), 9.27 (s, 1H); ^{13}C NMR (125 MHz, $CDCl_3$) δ 14.2, 22.2 (2C), 22.8 (2C), 26.1 (2C), 37.2 (2C), 42.2 (2C), 43.3 (2C), 43.5, 52.6 (m, 2C), 107.0 (d, J = 27.5 Hz), 115.0 (d, J = 3.75 Hz), 121.8 (d, J = 17.5 Hz), 131.6 (d, J = 6.25 Hz), 135.4 (d, J = 10.0 Hz), 157.5, 158.9, 161.3 (d, J = 242.5 Hz); HRMS (ESI), m/z calcd for $C_{24}H_{33}FN_3O_2$ (MH^-) 414.2554, found 414.2562.

4.1.18. N^1-(3-Chloro-4-methylphenyl)-N^2-(2,6-dicyclohexylpiperidin-4-yl)oxalamide (14b)

By use of a procedure similar to that described for the preparation of compound **8a**, the compound **7b** (120.5 mg, 0.500 mmol) was converted into the title compound **14b** (12.9 mg, 6% yield) as white powder.

^{1}H NMR (500 MHz, $CDCl_3$) δ 0.973 (t, J = 12.5 Hz, 2H), 1.18–1.86 (br, 20H), 2.11–2.19 (m, 2H), 2.35 (s, 3H), 4.09–4.21 (m, 1H), 7.20–7.22 (m, 1H), 7.30–7.32 (m, 1H), 7.35–7.37 (d, J = 2.50 Hz, 1H), 7.73 (m, 1H), 9.22 (s, 1H); ^{13}C NMR (125 MHz, $CDCl_3$) δ 19.6, 22.1 (2C), 22.7 (2C), 26.0 (2C), 29.7, 37.0, 42.1 (2C), 42.7 (2C), 43.2, 53.3 (2C), 118.0, 120.3, 131.2, 133.0, 134.7, 135.1, 157.5, 158.8; HRMS (ESI), m/z calcd for $C_{24}H_{33}ClN_3O_2$ (MH^+) 430.2267, found 430.2257.

4.1.19. N^1-(3-Bromo-4-methylphenyl)-N^2-(2,6-dicyclohexylpiperidin-4-yl)oxalamide (14c)

By use of a procedure similar to that described for the preparation of compound **8a**, the compound **7c** (142.0 mg, 0.500 mmol) was converted into the title compound **14c** (11.5 mg, 5% yield) as white powder.

^{1}H NMR (500 MHz, $CDCl_3$) δ 0.67–2.07 (br, 22H), 2.28 (br, 2H), 2.38 (s, 3H), 4.09–4.21 (m, 1H), 7.22 (d, J = 8.00 Hz, 1H), 7.28–7.38 (br, 1H), 7.43 (dd, J = 4.50, 2.50 Hz, 1H), 7.90 (d, J = 2.50 Hz, 1H), 9.21 (s, 1H); ^{13}C NMR (125 MHz, $CDCl_3$) δ 14.1, 22.1 (2C), 22.4 (2C), 22.7 (2C), 25.9, 30.0, 31.6, 36.9 (2C), 42.7 (3C), 52.7, 52.9, 118.6, 123.4, 125.0, 131.0, 134.9, 135.1, 157.4, 158.8; HRMS (ESI), m/z calcd for $C_{24}H_{33}BrN_3O_2$ (MH^+) 474.1762, found 474.1746.

4.2. Antiviral assay and cytotoxicity assay

Anti-HIV activity and cytotoxicity measurements in PM1/CCR5 cells (Yoshimura et al., 2010) were based on viability of cells that

had been infected or not infected with 100 TCID50 of an R5 primary isolate YTA48P exposed to various concentrations of the test compound. After the PM1/CCR5 cells were incubated at 37 °C for 7 days. The 50% inhibitory concentration (IC_{50}) values and the 50% cytotoxic concentration (CC_{50}) were then determined using the Cell Counting Kit-8 assay (Dojindo Laboratories). All assays were performed in duplicate or triplicate.

4.3. FACS analysis

JR-FL (R5, Sub B) chronically infected PM1 cells were pre-incubated with 0.5 μg/mL of sCD4 or 100 μM of a CD4 mimic for 15 min, and then incubated with an anti-HIV-1 mAb, 4C11, at 4 °C for 15 min. The cells were washed with PBS, and fluorescein isothiocyanate (FITC)-conjugated mouse anti-human IgG antibody was used for antibody-staining. Flow cytometry data for the binding of 4C11 (green lines) to the Env-expressing cell surface in the presence of a CD4 mimic are shown among gated PM1 cells along with a control antibody (anti-human CD19: black lines). Data are representative of the results from a minimum of two independent experiments. The number at the bottom of each graph shows the mean fluorescence intensity (MFI) of the antibody 4C11.

4.4. Molecular modeling

Dockings of compounds **3** and **13a** were performed using Molecular Operating Environment modeling package (MOE 2008. 10, Canada), into the crystal structure of gp120 (PDB, entry 3TGS).

Acknowledgements

This work was supported in part by Grant-in-Aid for Scientific Research from the Ministry of Education, Culture, Sports, Science, and Technology of Japan, and Health and Labour Sciences Research Grants from Japanese Ministry of Health, Labor, and Welfare. We are grateful to Professor Yoshio Hayashi and Dr. Fumika Yakushiji, Tokyo University of Pharmacy and Life Sciences for their assistance in the molecular modelings.

Supplementary data

Supplementary data (NMR charts of compounds) associated with this article can be found, in the online version, at http://dx.doi.org/10.1016/j.bmc.2013.02.041.

References and notes

1. Chan, D. C.; Kim, P. S. *Cell* **1998**, *93*, 681.
2. (a) Kadow, J.; Wang, H.-G.; Lin, P.-F. *Curr. Opin. Investig. Dugs* **2006**, *7*, 721; (b) Repik, A.; Clapham, P. R. *Structure* **2008**, *16*, 1603.
3. Holz-Smith, S.; Sun, I. C.; Jin, L.; Matthews, T. J.; Lee, K. H.; Chen, C. H. *Antimicrob. Agents Chemother.* **2001**, *45*, 60.
4. Lin, P.-F.; Blair, W.; Wang, T.; Spicer, T.; Guo, Q.; Zhou, N.; Gong, Y.-F.; Wang, H.-F. H.; Rose, R.; Yamanaka, G.; Robinson, B.; Li, C.-B.; Fridell, R.; Deminie, C.; Demers, G.; Yang, Z.; Zadjura, L.; Meanwell, N.; Colonno, R. *Proc. Natl. Acad. Sci. U.S.A.* **2003**, *100*, 11013.
5. Zhao, Q.; Ma, L.; Jiang, S.; Lu, H.; Liu, S.; He, Y.; Strick, N.; Neamati, N.; Debnath, A. K. *Virology* **2005**, *339*, 213.
6. (a) Madani, N.; Schön, A.; Princiotto, A. M.; LaLonde, J. M.; Courter, J. R.; Soeta, T.; Ng, D.; Wang, L.; Brower, E. T.; Xiang, S.-H.; Do Kwon, Y.; Huang, C.-C.; Wyatt, R.; Kwong, P. D.; Freire, E.; Smith, A. B., III; Sodroski, J. *Structure* **2008**, *16*, 1689; (b) LaLonde, J. M.; Elban, M. A.; Courter, J. R.; Sugawara, A.; Soeta, T.; Madani, N.; Princiotto, A. M.; Kwon, Y. D.; Kwong, P. D.; Schön, A.; Freire, E.; Sodroski, J.; Smith, A. B., III *Bioorg. Med. Chem. Lett.* **2011**, *20*, 354; (c) LaLonde, J. M.; Kwon, Y. D.; Jones, D. M.; Sun, A. W.; Courter, J. R.; Soeta, T.; Kobayashi, T.; Princiotto, A. M.; Wu, X.; Schön, A.; Freire, E.; Kwong, P. D.; Mascola, J. R.; Sodroski, J.; Madani, N.; Smith, A. B., III *J. Med. Chem.* **2012**, *55*, 4382.
7. Curreli, F.; Choudhury, S.; Pyatkin, I.; Zagorodnikov, V. P.; Bulay, A. K.; Altieri, A.; Kwon, Y. D.; Kwon, P. D.; Debnath, A. K. *J. Med. Chem.* **2012**, *55*, 4764.
8. (a) Yamada, Y.; Ochiai, C.; Yoshimura, K.; Tanaka, T.; Ohashi, N.; Narumi, T.; Nomura, W.; Harada, S.; Matsushita, S.; Tamamura, H. *Bioorg. Med. Chem. Lett.* **2010**, *20*, 354; (b) Narumi, T.; Ochiai, C.; Yoshimura, K.; Harada, S.; Tanaka, T.; Nomura, W.; Arai, H.; Ozaki, T.; Ohashi, N.; Matsushita, S.; Tamamura, H. *Bioorg. Med. Chem. Lett.* **2010**, *20*, 5853; (c) Narumi, T.; Arai, H.; Yoshimura, K.; Harada, S.; Nomura, W.; Matsushita, S.; Tamamura, H. *Bioorg. Med. Chem.* **2011**, *19*, 6735.
9. (a) Schön, A.; Madani, N.; Klein, J. C.; Hubicki, A.; Ng, D.; Yang, X.; Smith, A. B., III; Sodroski, J.; Freire, E. *Biochemistry* **2006**, *45*, 10973; (b) Schön, A.; Lam, S. Y.; Freire, E. *Future Med. Chem.* **2011**, *3*, 1129.
10. Yoshimura, K.; Harada, S.; Shibata, J.; Hatada, M.; Yamada, Y.; Ochiai, C.; Tamamura, H.; Matsushita, S. *J. Virol.* **2010**, *84*, 7558.
11. Kwon, Y. D.; Finzi, A.; Wu, X.; Dogo-Isonagie, C.; Lee, L. K.; Moore, L. R.; Schmidt, S. D.; Stuckey, J.; Yang, Y.; Zhou, T.; Zhu, J.; Vicic, D. A.; Debnath, A. K.; Shapiro, L.; Bewley, C. A.; Mascola, J. R.; Sodroski, J. G.; Kwong, P. D. *Proc. Natl. Acad. Sci. U.S.A.* **2012**, *109*, 5663.
12. (a) Kwong, P. D.; Wyatt, R.; Robinson, J.; Sweet, R. W.; Sodroski, J.; Hendrickson, W. A. *Nature* **1998**, *393*, 648; (b) Kwong, P. D.; Wyatt, R.; Mcajeed, S.; Robinson, J.; Sweet, R. W.; Sodroski, J.; Hendrickson, W. A. *Structure* **2000**, *8*, 1329.
13. McFarland, C.; Vicic, D. A.; Debnath, A. K. *Synthesis* **2006**, 807.
14. Sakai, K.; Yamada, K.; Yamasaki, T.; Kinoshita, Y.; Mito, F.; Utsumi, H. *Tetrahedron* **2010**, *66*, 2311.

frontiers in MICROBIOLOGY

ORIGINAL RESEARCH ARTICLE
published: 14 May 2013
doi: 10.3389/fmicb.2013.00117

Increased infectivity in human cells and resistance to antibody-mediated neutralization by truncation of the SIV gp41 cytoplasmic tail

Takeo Kuwata[1], Kaori Takaki[1], Ikumi Enomoto[1], Kazuhisa Yoshimura[2] and Shuzo Matsushita[1]*

[1] Center for AIDS Research, Kumamoto University, Kumamoto, Japan
[2] AIDS Research Center, National Institute of Infectious Diseases, Tokyo, Japan

Edited by:
Akio Adachi, The University of Tokushima Graduate School, Japan

Reviewed by:
Tetsuro Matano, University of Tokyo, Japan
Tsutomu Murakami, National Institute of Infectious Diseases, Japan
Hirofumi Akari, Kyoto University, Japan

***Correspondence:**
Shuzo Matsushita, Center for AIDS Research, Kumamoto University, 2-2-1 Honjo, Chuo-ku, Kumamoto 860-0811, Japan.
e-mail: shuzo@kumamoto-u.ac.jp

The role of antibodies in protecting the host from human immunodeficiency virus type 1 (HIV-1) infection is of considerable interest, particularly because the RV144 trial results suggest that antibodies contribute to protection. Although infection of non-human primates with simian immunodeficiency virus (SIV) is commonly used as an animal model of HIV-1 infection, the viral epitopes that elicit potent and broad neutralizing antibodies to SIV have not been identified. We isolated a monoclonal antibody (MAb) B404 that potently and broadly neutralizes various SIV strains. B404 targets a conformational epitope comprising the V3 and V4 loops of Env that intensely exposed when Env binds CD4. B404-resistant variants were obtained by passaging viruses in the presence of increasing concentration of B404 in PM1/CCR5 cells. Genetic analysis revealed that the Q733stop mutation, which truncates the cytoplasmic tail of gp41, was the first major substitution in Env during passage. The maximal inhibition by B404 and other MAbs were significantly decreased against a recombinant virus with a gp41 truncation compared with the parental SIVmac316. This indicates that the gp41 truncation was associated with resistance to antibody-mediated neutralization. The infectivities of the recombinant virus with the gp41 truncation were 7,900-, 1,000-, and 140-fold higher than those of SIVmac316 in PM1, PM1/CCR5, and TZM-bl cells, respectively. Immunoblotting analysis revealed that the gp41 truncation enhanced the incorporation of Env into virions. The effect of the gp41 truncation on infectivity was not obvious in the HSC-F macaque cell line, although the resistance of viruses harboring the gp41 truncation to neutralization was maintained. These results suggest that viruses with a truncated gp41 cytoplasmic tail were selected by increased infectivity in human cells and by acquiring resistance to neutralizing antibody.

Keywords: SIV, gp41, truncation, infectivity, resistance, neutralization, antibody

INTRODUCTION

The RV144 trial demonstrated 31% vaccine efficacy for preventing human immunodeficiency virus type 1 (HIV-1) infection (Rerks-Ngarm et al., 2009). Antibodies against the HIV-1, particularly against the V1/V2 loops, correlate inversely with infection risk (Haynes et al., 2012). Further recent isolation of monoclonal antibodies (MAbs) that neutralize a broad range of HIV-1 strains suggest the possibility for developing a vaccine that can induce cross-neutralizing antibodies effective for various HIV-1 strains (Kwong and Mascola, 2012). Although non-human primate models of simian immunodeficiency virus (SIV) infection can facilitate the evaluation of immunogens, epitopes and immune correlates, no potent and broad neutralizing MAb against SIV had been available.

To understand the mechanisms involved in neutralization of infectivity by antibodies in an SIV model, we recently isolated MAb B404 from a SIVsmH635FC-infected rhesus macaque, which potently and broadly neutralizes various SIV strains, such as SIVsmE543-3, SIVsmE660 and the neutralization-resistant variants, genetically diverse SIVmac316, and highly neutralization-resistant SIVmac239 (Kuwata et al., 2011). The B404 epitope, which comprises the V3 and V4 loops of Env and is intensely exposed by ligation of Env to CD4, is the target for potent and broad neutralization of SIV (Kuwata et al., 2013). Vigorous induction of B404-like neutralizing antibodies using the specific VH3 gene with a long complementarity-determining region 3 loop and λ light chain was observed in four SIVsmH635FC-infected macaques. The B404-resistant variants were induced by passaging viruses in the presence of increasing concentrations of B404. Genetical analysis of the gp120 region of B404-resistant variants revealed that the mutations in the C2 region of Env were important for the resistance to antibody-mediated neutralization (Kuwata et al., 2013).

In the present study, we further analyzed B404-resistant variants and determined the precise region responsible for the resistance to antibody-mediated neutralization. Genetic analysis of viruses during passage in the presence of B404 as well as phenotypic analysis using recombinant viruses revealed that a truncation of the gp41 cytoplasmic tail was the primary step leading to escape from neutralization.

MATERIALS AND METHODS

CELLS

PM1 (Lusso et al., 1995), PM1/CCR5 (Yusa et al., 2005), and HSC-F (Akari et al., 1999) cells were maintained in Roswell Park Memorial Institute (RPMI) 1640 medium containing 10% fetal bovine serum (FBS). TZM-bl (Platt et al., 1998; Derdeyn et al., 2000; Wei et al., 2002; Takeuchi et al., 2008) and 293T (DuBridge et al., 1987) cells were maintained in Dulbecco's modified Eagle's medium containing 10% FBS.

GENETIC ANALYSIS OF B404-RESISTANT VARIANTS

The induction of variants resistant to Fab-B404 (Kuwata et al., 2011) from SIVmac316 (Mori et al., 1992) harboring full-length gp41 was performed as described previously (Yoshimura et al., 2006; Hatada et al., 2010; Kuwata et al., 2013). Briefly, 5,000 $TCID_{50}$ (50% tissue culture infectious dose) SIVmac316 was incubated with 5 ng/ml Fab-B404 for 30 min at 37°C. Then, 5×10^4 PM1/CCR5 cells were added to the virus–Fab mixture. After incubation for 5 h, cells were washed with phosphate-buffered saline (PBS) and resuspended in RPMI 1640 supplemented with 10% FBS without Fab-B404. The culture supernatant was harvested 7 days later and used to infect fresh PM1/CCR5 cells for the next round of culture in the presence of increasing concentrations of Fab-B404. Proviral DNA samples were extracted from cells using a QIAamp DNA Blood Mini Kit (QIAGEN, Hilden, Germany) after 8, 17, 20, 23, and 26 passages as well as from P26C cells obtained after 26 passages in the absence of Fab-B404. The gp120 region was amplified using Platinum Taq DNA Polymerase High Fidelity (Invitrogen, Carlsbad, CA, USA) with primers SEnv-F (5′-ATG GGA TGT CTT GGG AAT CAG C-3′) and SER1 (5′-CCA AGA ACC CTA GCA CAA AGA CCC-3′). The whole *env* gene was amplified with primers SRev-F (5′-GGT TTG GGA ATA TGC TAT GAG-3′) and SEnv-R (5′-CCT ACT AAG TCA TCA TCT T-3′). The polymerase chain reaction (PCR) products were cloned using a TA cloning kit (Invitrogen), and subjected to sequencing. Nucleotide sequences were aligned and analyzed phylogenetically using Molecular Evolutionary Genetics Analysis version 5 (MEGA5) (Tamura et al., 2011).

CONSTRUCTION OF INFECTIOUS MOLECULAR CLONES WITH THE Env REGION FROM B404-RESISTANT VARIANTS

One of the clones from passage 26, P26B404 clone 26, was selected for construction of recombinant viruses, because this clone had mutations typical of the major population of P26B404 variants. Infectious molecular clones SS, SN, and NS were generated by replacing fragments *Sph*I–*Sac*I [nucleotides (nt) 6,446–9,226], *Sph*I–*Nhe*I (nt 6,446–8,742), and *Nhe*I–*Sac*I (nt 8,742–9,226) with the corresponding regions of SIVmac316, respectively. Mutants F277V and N295S, which have point mutations at amino acid residues 277 and 295 of Env, respectively, were constructed by PCR mutagenesis using the SIVmac316 plasmid as template. The changes from phenylalanine (TTC) to valine (GTC) in F277V and asparagine (AAT) to serine (AGT) in N295S were introduced using primers F277VFw (5′-TTG GTT TGG CGT CAA TGG TAC TAG GGC-3′), F277VRv (5′-GTA CCA TTG ACG CCA AAC CAA G-3′), N295SFw (5′-GGC AAT AGT AGT AGA ACC ATA ATT AG-3′), and N295SRv (5′-AAT TAT GGT TCT ACT ACT ATT GCC-3′). Mutant and parental SIVmac316 plasmids were transfected into 293T cells using X-tremeGENE 9 DNA Transfection Reagent (Roche Molecular Biochemicals, Mannheim, Germany). After 2 days, the supernatants containing viruses were filtered (0.45 μm) and stored at −80°C.

ANALYSIS OF VIRAL INFECTIVITY

For determination of $TCID_{50}$ in PM1 and PM1/CCR5 cells, 5×10^4 cells in 50 μl were inoculated with 50 μl serially diluted virus stocks in a 96-well plate and cultured for 2 weeks. Virus replication was judged by observation of cytopathic effects (CPE) by light microscopy. The $TCID_{50}$ in TZM-bl cells was determined by measuring luciferase activities. Briefly, 100 μl medium, 50 μl serially diluted virus stock, and 50 μl 1×10^4 cells containing 37.5 μg/ml diethylaminoethyl (DEAE) dextran were added to the wells of a 96-well plate. The plate was then incubated at 37°C for 2 days. After washing with PBS, cells were lysed with 30 μl cell lysing buffer (Promega, Madison, WI, USA) for 15 min at room temperature (RT) and then 10 μl of cell lysate was transferred to a 96-well white solid plate (Coster, Cambridge, MA, USA). Luciferase activity was measured using a Centro XS3 LB960 microplate luminometer (Berthold Technologies, Bad Wildbad, Germany) and a luciferase assay system (Promega). The $TCID_{50}$ was calculated according to the formula of Reed and Muench (1938).

Infectivity of viruses in PM1, PM1/CCR5, and HSC-F cells was evaluated by detecting infected cells using flow cytometry as described previously (Kuwata et al., 2011). Briefly, PM1 and PM1/CCR5 cells were adjusted to 1×10^6 cells/ml and HSC-F cells were adjusted to 5×10^6 cells/ml. Aliquots of 100 μl cells per well in a 24-well plate were inoculated with 100 μl of diluted virus stocks. After incubation for 6 h, 800 μl fresh medium was added to wells. One-half of the cells in each well were collected at 4, 7, and 10 days post-inoculation. Cells were washed with PBS and fixed with IC Fixation Buffer (eBioscience, San Diego, CA, USA). After washing with Permeabilization Buffer (eBioscience) twice, the cells were intracellularly stained with 4 μg/ml (50 μl) anti-p27 Fab, B450 (Kuwata et al., 2011) by incubation for 20 min at RT. The cells were then incubated with 50 μl anti-HA antibody (1:200; 3F10, Roche Molecular Biochemicals) for 20 min at RT followed by incubation with 50 μl of anti-rat-FITC (1:500; Santa Cruz Biotechnology, Santa Cruz, CA, USA) for 20 min at RT. The stained cells were analyzed using a FACSCalibur (BD Biosciences, Franklin Lakes, NJ, USA). Frequencies of infected cells were determined by comparison with an uninfected control. Data analysis was performed using FlowJo (TreeStar, San Carlos, CA, USA).

All infectivity experiments were performed at least twice and the representative results are shown.

ANALYSIS OF NEUTRALIZING ACTIVITIES

The Fab clones B404 and K8, isolated from an SIV-infected macaque (Kuwata et al., 2011), and murine MAb M318T (Matsumi et al., 1995) were used to examine the sensitivity of viruses to antibody-mediated neutralization in TZM-bl cells as described previously (Kuwata et al., 2011). Briefly, 100 μl serially diluted antibodies in duplicate were incubated with 200 $TCID_{50}$ (50 μl) of virus in a 96-well plate. After incubation for 1 h at 37°C, 100 μl

of 1×10^5 TZM-bl cells/ml containing 37.5 μg/ml DEAE dextran were added. After incubation for 2 days, luciferase activities were measured as described above for the analysis of viral infectivity. The 50% inhibitory concentrations (IC_{50}) and maximal percent of inhibition (MPI) were calculated from the average values by non-linear regression using Prism5 (GraphPad Software, San Diego, CA, USA).

Sensitivity to neutralization by B404 in macaque cells was analyzed using HSC-F cells, a cynomolgus macaque cell line immortalized by infection with *Herpesvirus saimiri* (Akari et al., 1999). Fab-B404 was serially diluted and 50 μl aliquots were mixed with 50 μl undiluted or 10-fold diluted virus in a 96-well plate. After 1 h incubation at 37°C, 2×10^5 cells in 100 μl were added to each well and cultured for 1 day. The infected cells were washed twice with PBS, resuspended in 200 μl fresh medium, and cultured in a new 96-well plate. Viral infection was examined 4 days post-inoculation by intracellular staining of p27, as described above for the analysis of viral infectivity. Infectivity was determined in duplicate and the average value was used for the analysis of neutralization.

All neutralizing assays were performed at least twice and the representative results are shown.

WESTERN BLOTTING ANALYSIS OF VIRAL PROTEINS

Cells and supernatants were collected from six-well plate 2 days after transfection of 293T cells with infectious molecular clones, as previously described (Yuste et al., 2005). Supernatants were filtered (0.45 μm) and clarified by centrifugation for 10 min at 3,000 rpm. The clarified supernatants were centrifuged at 13,200 rpm for 90 min at 4°C, and the viral pellets were resuspended in 1 ml PBS and centrifuged again. Pellets were then dissolved in 80 μl sample buffer [62.5 mM Tris–HCl, pH 6.8, 2% sodium dodecyl sulfate (SDS), 25% glycerol, 5% 2-mercaptoethanol, 0.01% bromophenol blue]. Cells were washed with PBS and lysed in 300 μl sample buffer. Samples of virions and cell lysates were boiled for 5 min, and the proteins were separated by SDS-polyacrylamide gel electrophoresis using SuperSep Ace 5–20% (Wako Pure Chemical Industries, Osaka, Japan). Proteins were transferred to an Immun-Blot PVDF Membrane (Bio-Rad Laboratories, Hercules, CA, USA). The membrane was blocked with 5% skim milk TBS-T (Tris-buffered saline containing 0.1% Tween 20) for 1 h at RT, and then washed three times with TBS-T. For the detection of gp120, the membrane was incubated overnight at 4°C with 1 μg/ml M318T (Matsumi et al., 1995) in 5% skim milk TBS-T. After washing three times with TBS-T, the membrane was incubated with anti-mouse immunoglobulin G (IgG) peroxidase (1:4,000, Santa Cruz Biotechnology) for 1 h at RT. The membrane was washed three times with TBS-T and once with TBS, and then TMB solution (KPL, Gaithersburg, MD, USA) was added to develop color. Viral proteins gp41 and p26 were similarly examined using crude supernatants from bacterial culture producing B408 and B450 (Kuwata et al., 2011), which were mixed with the same amount of 5% skim milk TBS-T. The membrane was incubated with anti-HA-HRP antibody (1:1,000; Roche Molecular Biochemicals) and Chemi-Lumi One L (Nacalai Tesque, Kyoto, Japan), and viral proteins were visualized using ImageQuant LAS 4000 (GE Healthcare, Piscataway, NJ, USA)

RESULTS

EVOLUTION OF VIRUSES DURING PASSAGE UNDER THE PRESSURE OF Fab-B404

To select for variants resistant to MAb B404, an antibody that targets a conformational epitope comprising the gp120 V3 and V4 loops, we passaged SIVmac316 that possesses a full-length gp41 in PM1/CCR5 cells in the presence of increasing concentrations of Fab-B404. The virus recovered at passage 26 (P26B404) was resistant to neutralization by B404 (V3/V4) and other antibodies, MAbs K8 (CD4i) and M318T (V2), that target epitopes other than that recognized by B404 (Kuwata et al., 2013). The region covering the whole *env* gene were amplified by PCR and cloned from viruses at passage 8, 17, 20, 23, and 26. The nucleotide sequences were phylogenetically analyzed to show the evolution of B404-resistant variants (**Figure 1**). The first major mutation was a change from glutamine (CAG) to a stop codon (TAG) at 733rd amino acid residue of Env. The Q733stop substitution in the gp41 cytoplasmic domain was observed in 12 of 14 clones at passage 8 and in all clones thereafter. Another stop codon (W782stop) was the second

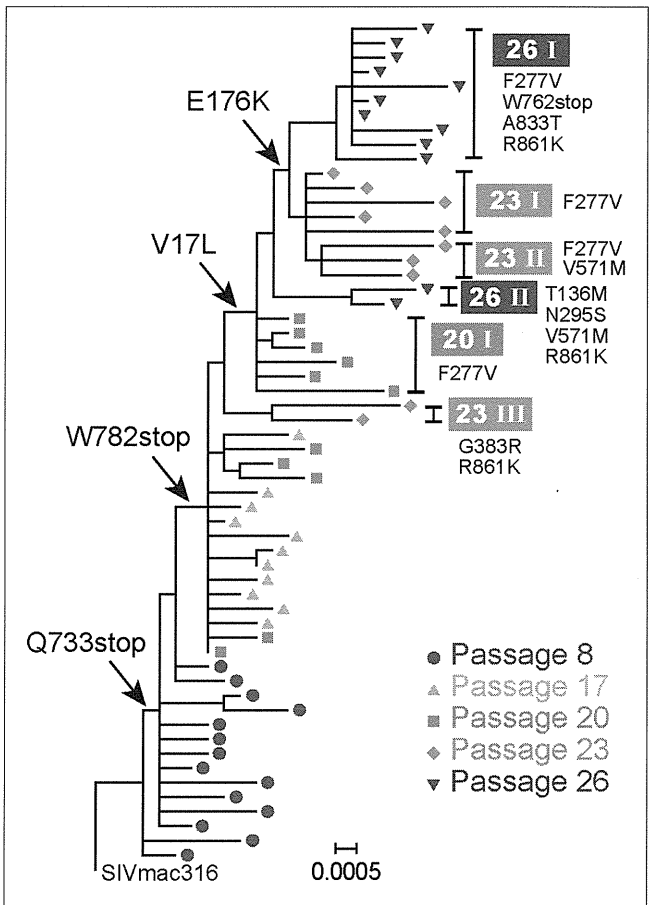

FIGURE 1 | Evolution of B404-resistant variants. Nucleotide sequences of the *env* gene, which were derived from proviruses at passages 8, 17, 20, 23, and 26, were phylogenetically analyzed using MEGA5. Arrows indicate major substitutions as follows: Q733stop, W782stop, V17L, and E176K. Clones with representative amino acid substitutions were separated into groups, which are shown on the right side along with the corresponding substitutions.

major mutation, which was detected after 17 passages. Substitutions V17L in the signal peptide and E176K in the V2 loop emerged after 20 and 23 passages, respectively, although the E176K substitution was also observed in P26C, control viruses after 26 passages in the absence of B404 (**Table 1**). In addition to these substitutions, most of clones acquired the F277V substitution in the late stage of evolution, except for one group at passage 26 which has the N295S substitution (see **Figure 1**, group 26II). Group 26II was clearly distinguished from group 26I by amino acid substitutions, such as T136M, N295S, and D571M/E (**Table 1**), suggesting two lineages of variants in P26B404.

These results demonstrated that the first step in acquiring resistance to B404 was the truncation of gp41. Although substitutions in gp120, represented by F277V, might contribute to the resistance to a high concentration of B404, 20 passages were required for the emergence of these substitutions.

Table 1 | Frequency* of amino acid substitutions in Env clones from B404-resistant variants after 26 passages.

Substitution	Region	P26B404		P26C
		I	II	
	gp120	**(*n* = 22)**	**(*n* = 8)**	**(*n* = 14)**
V17L	Signal peptide	**100%**	**100%**	0.0%
G62S	C1	0.0%	0.0%	21.4%
M67V/L/T	C1	4.5%	0.0%	21.4%
A68T	C1	0.0%	0.0%	**92.9%**
T136M	V1	4.5%	**87.5%**	0.0%
T137I	V1	0.0%	0.0%	14.3%
K141E/R	V1	0.0%	12.5%	7.1%
E176K	V2	**90.9%**	12.5%	35.7%
F277V	C2	**100%**	0.0%	0.0%
N295S	C2	0.0%	**100%**	0.0%
Q341H	V3	13.6%	12.5%	14.3%
D374N	C3	0.0%	0.0%	28.6%
K403R	V4	0.0%	12.5%	7.1%
W441R	C4	4.5%	0.0%	7.1%
	gp41	**(*n* = 10)**	**(*n* = 2)**	**(*n* = 7)**
F528S/L	Extracellular	20.0%	0.0%	0.0%
D571M/E	Extracellular	10.0%	**100%**	0.0%
Q733stop	Cytoplasmic	**100%**	**100%**	0.0%
W762stop	Cytoplasmic	**100%**	0.0%	0.0%
W782stop	Cytoplasmic	**100%**	0.0%	0.0%
A833T	Cytoplasmic	**90.0%**	0.0%	0.0%
R839K	Cytoplasmic	0.0%	0.0%	**57.1%**
R861K	Cytoplasmic	**100%**	**100%**	0.0%

Percentages of substitutions in populations P26B404 and P26C, which were obtained after 26 passages in the presence and absence of B404, respectively, are shown. The P26B404 population is separated into two subpopulations according to the phylogenetic analysis in **Figure 1. All the substitutions that are observed in more than one clone are shown here. Boldface indicates substitutions dominant (>50%) in each population. The numbers of clones analyzed for the gp120 and gp41 regions are shown in parentheses.*

TRUNCATION OF gp41 CONFERRED RESISTANCE TO ANTIBODY-MEDIATED NEUTRALIZATION

To analyze effect of substitutions in B404-resistant variants on resistance to neutralization, recombinant viruses were constructed (**Figure 2**). The *env* region of SIVmac316 was replaced by that of P26B404 clone 26, which had substitutions typical to the P26I group. The resultant molecular clones SS, SN, and NS had substitutions in the entire *env* region, gp120 and gp41 from P26B404I, respectively. SS and NS were predicted to have a truncated gp41 with no other mutation in gp41, because the Q733stop substitution was the first substitution in gp41. Point mutants with substitutions F277V and N295S, which were representative mutations at late passages, were also constructed by PCR mutagenesis.

These mutant viruses were examined for their sensitivity to neutralization by three MAbs B404 (V3/V4 conformational), K8 (CD4i), and M318T (V2). The neutralization of SS that contain the entire *env* region from P26B404I was similar to those of P26B404, indicating that the *env* region is responsible for the

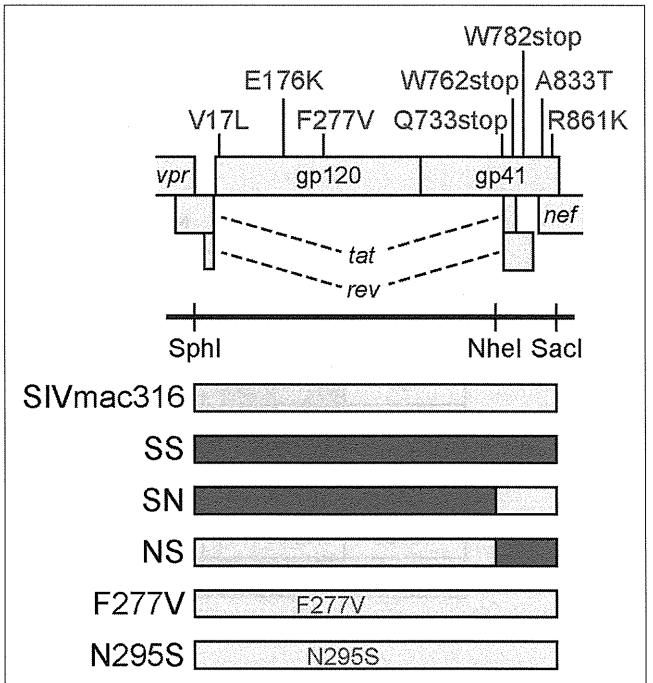

FIGURE 2 | Construction of infectious SIV clones with B404-resistant mutations. The open reading frames of the SIV genome are shown along with the Env substitutions in the B404-resistant variant typical to P26B404I. Full-length SIV clones were constructed from parental SIVmac316 by replacing the *env* region with that of the B404-resistant variant (blue) using *Sph*I, *Nhe*I, and *Sac*I sites. The resultant virus SS contains all of the Env substitutions present in P26B404I. Viruses SN and NS contain substitutions in gp120 and gp41, respectively. Point mutants F277V and N295S were constructed by inserting the substitutions F277V and N295S into SIVmac316, respectively.

resistance to neutralization (**Figure 3A**). Recombinants SN and NS, which have substitutions in gp120 and gp41 from P26B404I, respectively, showed varying degrees of resistance. The IC_{50} values of SN and NS against B404 were intermediates between the parental SIVmac316 and the neutralization-resistant P26B404. Maximal inhibition reached a plateau at 73.8, 82.3, and 81.9% in SS, NS, and P26B404, respectively, but the MPI value of SN (94.9%) was close to that of SIVmac316 (100%; **Figure 3B**). Neutralization resistance to anti-CD4i MAb K8 was characterized by decreases in the IC_{50} value of SN and the MPI of NS. Neutralization by anti-V2 MAb M318T was even enhanced in SN, although NS showed the resistance comparable to those of SS and P26B404. The decreases in MPI values were commonly observed for the neutralization of NS by the three MAbs (**Figure 3B**). Resistance to neutralization was not significantly detected by the point mutants F277V and N295S, except for the neutralization of F277V by K8 (4.3-fold decrease of IC_{50} value). These results indicated that the entire *env* region, including substitutions in both gp120 and gp41, was responsible for the full-resistance of P26B404 to neutralization. The decrease of MPI values for NS suggested that truncation of gp41 by the Q733stop substitution, the first major substitution in viral evolution, was important to escape from the neutralizing antibodies.

INCREASED INFECTIVITY FOR HUMAN CELLS BY SIV WITH A TRUNCATED gp41

Truncation of gp41 in SIV is associated with the adaptation to human cells (Hirsch et al., 1989; Kodama et al., 1989), which may partially contribute to neutralization resistance (Yuste et al., 2005). To explore the mechanism of neutralization resistance of P26B404, the infectivity of recombinant viruses was analyzed by determining the $TCID_{50}$ values of virus stocks prepared by transfection of 293T cells (**Table 2**). The $TCID_{50}$ values in all the human cells tested were significantly higher for SS and NS viruses with truncated gp41 than

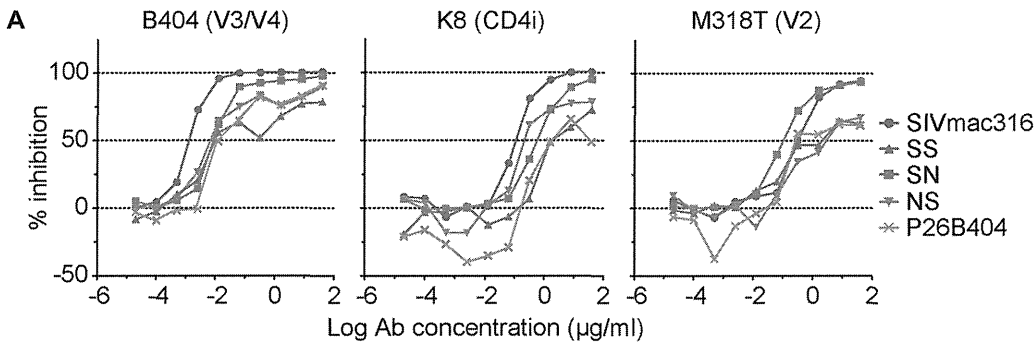

B

Neutralization profile of mutant viruses

Virus	B404 (V3/V4)		K8 (CD4i)		M318T (V2)	
	IC_{50}	MPI	IC_{50}	MPI	IC_{50}	MPI
SIVmac316	1.3E-03 (1.0)	100 (0.0)	1.1E-01 (1.0)	99.0 (0.0)	3.3E-01 (1.0)	94.3 (0.0)
SS	1.9E-02 (14.5)	73.8 (-26.2)	1.8E+00 (16.3)	67.9 (-31.1)	9.4E-01 (2.8)	65.5 (-28.8)
SN	9.1E-03 (6.8)	94.9 (-5.1)	5.9E-01 (5.3)	94.7 (-4.4)	1.0E-01 (0.3)	92.5 (-1.8)
NS	6.8E-03 (5.1)	82.3 (-17.7)	2.1E-01 (1.9)	77.0 (-22.0)	1.7E+00 (5.2)	67.6 (-26.7)
F277V	3.8E-03 (2.8)	100 (0.0)	4.8E-01 (4.3)	99.6 (0.5)	3.0E-01 (0.9)	94.8 (0.5)
N295S	2.3E-03 (1.7)	99.6 (-0.4)	1.4E-01 (1.2)	99.9 (0.8)	3.1E-01 (0.9)	97.0 (2.7)
P26B404	1.7E-02 (12.5)	81.9 (-18.1)	8.2E-01 (7.3)	54.6 (-44.5)	2.5E-01 (0.8)	60.0 (-34.3)

Fold change of IC_{50}
> 10
3-10
< 3

% change of MPI
< -20
-10- to -20
> -10

FIGURE 3 | Sensitivities of viruses with B404-resistant mutations to neutralization by MAbs. (A) Sensitivities of mutant viruses SS, SN, and NS to neutralization by MAbs Fab-B404 (anti-V3/V4), Fab-K8 (anti-CD4i), and M318T (anti-V2) are shown. Neutralization of parental SIVmac316 and B404-resistant P26B404 is also shown as controls sensitive and resistant to neutralization, respectively. **(B)** The sensitivities to neutralization are represented by values for IC_{50} (μg/ml) and MPI (%). Viruses were examined for their sensitivities to neutralization by MAbs Fab-B404, Fab-K8, and M318T in TZM-bl cells. The IC_{50} and MPI values were determined using Prism 5. The fold-change of IC_{50} was calculated by dividing the IC_{50} value by that of the parental SIVmac316. Percent change of MPI was calculated by subtracting the MPI value from that of SIVmac316. These changes are shown in parentheses and significant changes are indicated by magenta (IC_{50}: >10; MPI: < −20) and orange (IC_{50}: 3–10; MPI: −20 to −10) highlighting.

parental SIVmac316 and SN, in which gp41 is intact. In particular, NS showed a striking increase in $TCID_{50}$ values, which were 7,100-, 1,000-, and 140-fold higher than those of parental SIVmac316 in PM1, PM1/CCR5, and TZM-bl cells, respectively. These results indicate that truncation of gp41 caused by the Q733stop substitution increases viral infectivity for human cells.

To compare viral infectivity in human and macaque cells, viral infection was monitored after inoculation of PM1 and PM1/CCR5 human cells and the HSC-F cynomolgus macaque cell line with varying dilutions of virus stocks (**Figure 4**). Consistent with the $TCID_{50}$ analysis, a higher frequency of infected cells was detected earlier in PM1 and PM1/CCR5 cells inoculated with NS than the parental SIVmac316. In contrast, SN showed decreased infectivity in PM1 and PM1/CCR5 cells, apparently because PM1 cells were not infected by a 1,000-fold diluted SN stock. Although the $TCID_{50}$ values of SS were much higher than those of SIVmac316, the replication kinetics of SS were similar to those of SIVmac316 in PM1 and PM1/CCR5 cells. These results suggest that gp41 truncation increases infectivity for human cells and that the substitutions in gp120 of P26B404I are associated with slow and poor replication compared with that of SIVmac316.

Infectivity for macaque cells was more significantly affected than that for human cells by the substitutions in gp120 of P26B404I (**Figure 4**, lower panels). Infected cells were detected in HSC-F cells inoculated with 1,000-fold diluted virus stocks of SIVmac316 and NS, but viral infection in HSC-F cells was limited to a low frequency even by inoculation with 10-fold diluted virus stocks of SS and SN. Truncation of gp41 did not significantly affect replication in HSC-F macaque cells, although truncation of gp41 was disadvantageous for replication in primary T cell cultures from macaques (Hirsch et al., 1989; Kodama et al., 1989).

These results demonstrate that gp41 truncation strikingly increases infectivity for human cells, but not for macaque cells, and that the substitutions in gp120 decrease infectivity in human and macaque cells. Truncation of gp41, which conferred extremely high infectivity for PM1/CCR5 cells, may be the first step to escape from neutralization and the substitutions in gp120 may be the second step to replicate in the presence of high concentration of B404.

Table 2 | Infectivity* of viruses with substitutions from P26B404.

Viruses	PM1	PM1/CCR5	TZM-bl
SIVmac316	4.2E+02 (1.0)	1.4E+03 (1.0)	9.6E+04 (1.0)
SS	2.9E+05 (710)	4.7E+05 (350)	6.3E+06 (66)
SN	2.0E+03 (4.8)	8.4E+03 (6.2)	2.9E+05 (3.1)
NS	2.9E+06 (7,100)	1.4E+06 (1,000)	1.4E+07 (140)

**Infectivity is shown by the $TCID_{50}$/ml values of the viruses, which were prepared by transfection of 293T cells, in PM1, PM1/CCR5, and TZM-bl cells. The fold-change, which was calculated by dividing the mutant $TCID_{50}$/ml value by that of the parental SIVmac316, is shown in the parentheses.*

INCREASED INCORPORATION OF Env INTO VIRIONS IN SIV WITH TRUNCATED gp41

Incorporation of Env into virions was examined using these recombinant viruses, because increased infectivity by gp41 truncation was suggested to be associated with the Env content of virions (Manrique et al., 2001; Zhu et al., 2003, 2006; Yuste et al., 2004, 2005). Analysis of viral proteins in cells and supernatants from transfected 293T cells revealed that incorporation of Env into virions was significantly high in SS and NS viruses with the Q733stop substitution (**Figure 5**). MAb to gp120 showed a higher amount

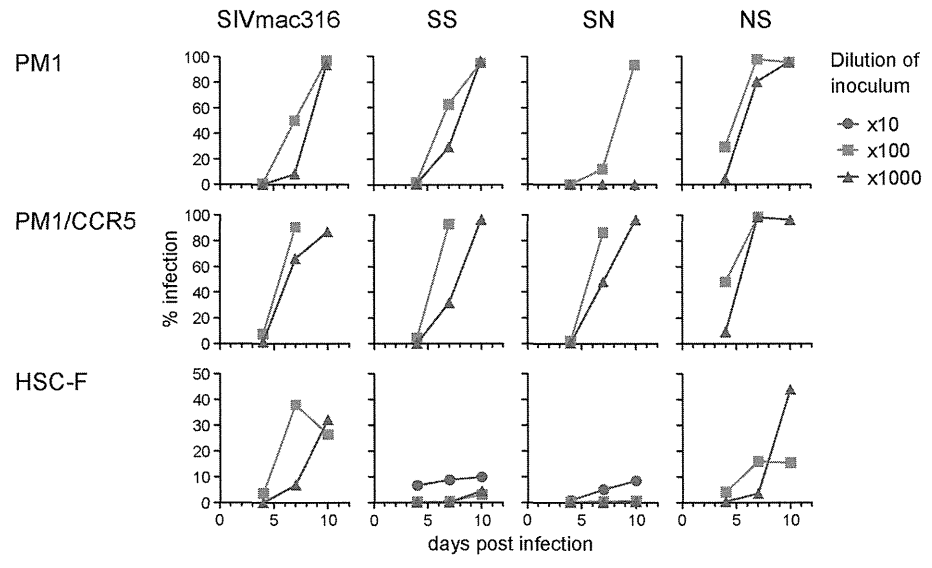

FIGURE 4 | Replication of B404-resistant viruses in human and macaque cells. Frequencies of infected cells at 4, 7, and 10 days post-infection are shown. PM1 and PM1/CCR5 human T cells and HSC-F cynomolgus macaque T cells were infected with the various dilutions of SIVmac316, SS, SN, and NS. Infected cells were detected using flow cytometry after intracellular staining by B450 (anti-p27 Fab).

of gp120 and gp160 in virions from SS and NS than those from SN and the parental SIVmac316, although the production of Env proteins in the transfected cells was at the same level among all the viruses (**Figure 5A**). MAb to gp41 also demonstrated that truncated gp41 was more abundant in virions compared with full-length gp41 (**Figure 5B**). Semi-quantification by densitometric scanning of gp41 and p26 images suggested that the levels of gp41 amount per virion in SS and NS were 12- and 44-fold higher than that of SIVmac316, respectively, after adjusting virion numbers using the p26 amounts. In contrast to the increased amount of Env proteins in virions from viruses with truncated gp41, the level of Gag p27 in virions was low in SS and NS compared with those in SN and SIVmac316 (**Figure 5C**). This indicates that the Env content per virion, which was normalized by the amount of p27, was significantly high in viruses with truncated gp41. These results suggest that truncation of gp41 by the Q733stop substitution enhances incorporation of Env into virions.

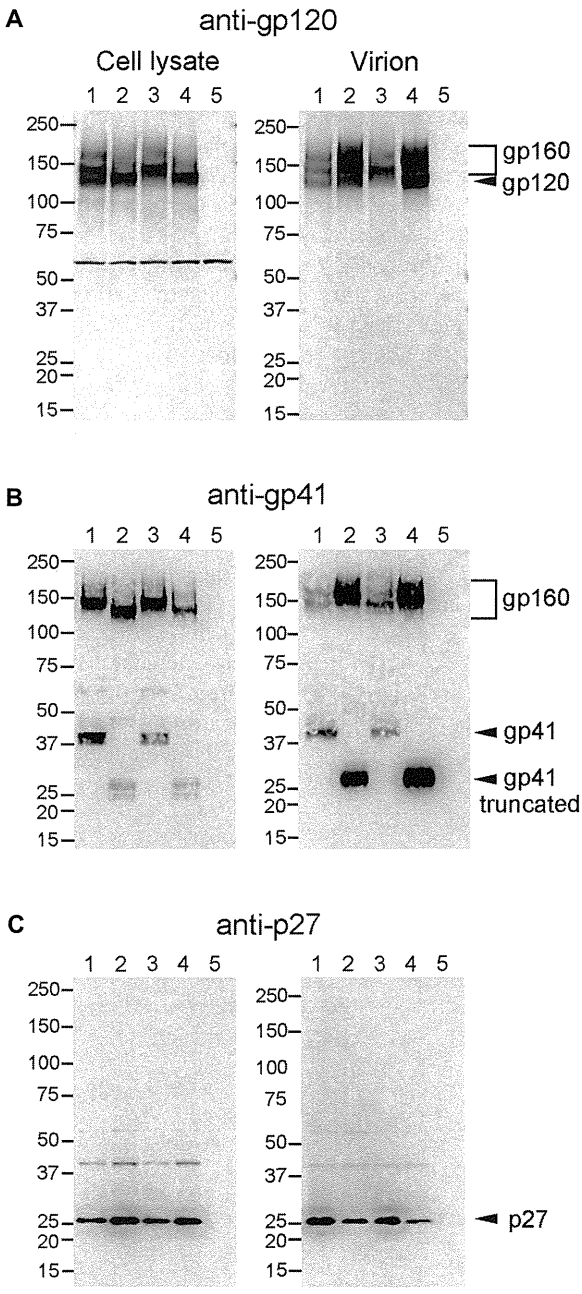

FIGURE 5 | Effect of B404-resistant mutations on the incorporation of Env into virions. Cell lysates (left panels) and virions (right panels) of SIVmac316 (lane 1), SS (lane 2), SN (lane 3), NS (lane 4), and mock-infected control (lane 5), which were prepared from transfected 293T cells, were analyzed by Western blotting. Viral proteins gp120 **(A)**, gp41 **(B)**, and p27 **(C)** were detected using MAbs M318T (anti-gp120 V2), B408 (anti-gp41 cluster I), and B450 (anti-p27), respectively.

NEUTRALIZATION RESISTANCE OF SIV WITH TRUNCATED gp41 IN MACAQUE CELLS

The analysis of infectivity of recombinant viruses suggested that the resistance to neutralization by truncation of gp41 might be due to adaptation to human cells. To examine this hypothesis, sensitivity to neutralization by B404 was determined in HSC-F macaque cells using SIVmac316 and NS, which showed similar infectivity for HSC-F cells (**Figure 4**). In flow cytometric analysis, infection in the presence or absence of B404 demonstrated that the high sensitivity of SIVmac316 and resistance of NS to neutralization were maintained in HSC-F cells (**Figure 6**). The frequency of infected cells decreased from 41.5% to the background level (2.03%) in inoculation with the undiluted stock of SIVmac316. In contrast, infection with NS, even with a 10-fold diluted virus stock, was significant in HSC-F cells in the presence of B404 (**Figure 6A**). Neutralization of NS in HSC-F cells was characterized by a decrease in maximal inhibition (**Figure 6B**), which was also observed in TZM-bl cells (**Figure 3A**). The magnitude of resistance of NS to B404 was greater when infection was performed using the undiluted stock compared with the 10-fold diluted stock, raising the possibility that B404 did not inhibit infection with a high titer of viruses. However, the resistance of NS was shown by infection with a low titer of NS, in which the frequency of infected cells in the absence of B404 (23.8%) was lower than infection with undiluted SIVmac316 (41.5%). Further, immunoblotting analysis revealed that the amount of virions was higher in the virus stock of SIVmac316 than that of NS (**Figure 5**).

These results indicate that gp41 truncation by the Q733stop substitution contributes to neutralization resistance of viruses in macaque cells. This suggests that the resistance to neutralization by truncation of gp41 is not due to the adaptation to human cells. The Q733stop substitution, the first major mutation during passages in the presence of B404, might be selected because it facilitates adaptation of virus to human cells and imparts resistance to antibody.

DISCUSSION

In the present study, truncation of the cytoplasmic tail of gp41, which was caused by the Q733stop substitution in Env, was the first major mutation detected during passage of SIV in the presence of the neutralizing antibody B404. Analysis of recombinant viruses suggested that the gp41 truncation was selected by their resistance to neutralizing antibody, which was characterized by the decrease of maximal inhibition compared with viruses with intact gp41, and

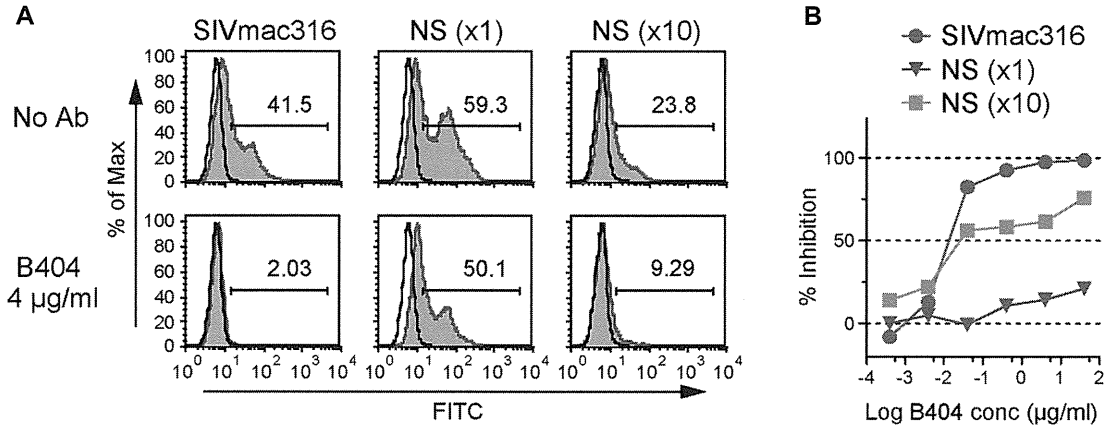

FIGURE 6 | Contribution of gp41 truncation to neutralization resistance in infection of macaque cells. (A) Infection of HSC-F cells in the presence (4 μg/ml) or absence of Fab-B404 is shown. HSC-F cells were inoculated with undiluted SIVmac316 and NS, and 10-fold diluted NS. Viral infection was monitored 4 days post-infection using flow cytometry after intracellular staining by B450 (anti-p27 Fab). **(B)** Neutralization of SIVmac316 and NS by B404 in HSC-F cells are shown. Percent inhibition was calculated by comparison with the infected culture in the absence of B404.

increased infectivity for human cells. The premature stop codon in the gp41 cytoplasmic region was frequently detected in SIV strains propagated in human cell culture *in vitro*, such as the original SIVmac316 clone, SIVmac1A11 and 17E-Fr (Hirsch et al., 1989; Kodama et al., 1989; Mori et al., 1992; Bonavia et al., 2005; Vzorov et al., 2005). The truncation of gp41 is considered as an adaptation of SIV to replication in human cell culture, because the premature stop codon rapidly reverted to express full-length gp41 after infection of rhesus primary cell culture *in vitro* and rhesus macaques *in vivo* (Hirsch et al., 1989; Kodama et al., 1989). Mutant viruses harboring the gp41 truncation showed increased infectivity for human cells, although the effects on infectivity varied depending on the SIV strain and the length of the gp41 truncation (Manrique et al., 2001; Yuste et al., 2004, 2005; Vzorov et al., 2005, 2007). The enhancement effect of gp41 truncation on incorporation of Env into virions, which were demonstrated by quantification of viral proteins in virions (Yuste et al., 2004) and electron tomography analysis of Env trimers on virions (Zhu et al., 2003, 2006), was partly associated with the increased infectivity caused by gp41 truncation (Manrique et al., 2001; Yuste et al., 2004, 2005). Because expression of Env on the cell surface is regulated by the cytoplasmic domain of gp41, truncation of gp41 may increase Env density on both cells and virions (LaBranche et al., 1995; Berlioz-Torrent et al., 1999; Postler and Desrosiers, 2013). Consistent with these studies, infectivity for human cells and Env incorporation into virions was enhanced by gp41 truncation in the present study. Although the mechanism responsible for increasing viral infectivity caused by gp41 truncation remains unclear, the high virion Env content may contribute to the efficient replication of viruses with truncated gp41 in human cells.

The effect of gp41 truncation on susceptibility to antibody-mediated neutralization is controversial, perhaps due to the SIV strains used for the analyses. Because most of prototypic SIV clones with truncated gp41 were macrophage-tropic, CD4-independent, and neutralization-sensitive (Mori et al., 1992; Bonavia et al., 2005; Vzorov et al., 2005), the truncation of gp41 was assumed responsible for the high sensitivity to neutralization. However, the resistance to neutralization by gp41 truncation was shown using the E767stop mutant of SIVmac316 (Yuste et al., 2005). This is consistent with our results using SIVmac316 harboring the Q733stop substitution, indicating that gp41 truncation contributes to resistance of SIVmac316 to neutralization. The increased infectivity of viruses with gp41 truncation in human cells may partially play a role in resistance by overcoming antibody-mediated neutralization via efficient attachment and entry of viruses to cells. However, we showed that gp41 truncation was also associated with neutralization resistance in macaque cells, in which gp41 truncation did not significantly affect infectivity. This suggests that the increased infectivity in human cells does not significantly affect the neutralization resistance of viruses with truncated gp41. As shown by provision of excess Env in trans, high Env content in virions may be critical for antibody-mediated neutralization (Yuste et al., 2005). Further studies will be required to understand the mechanism of resistance to neutralization conferred by gp41 truncation.

In the present study, we demonstrated that truncation of the cytoplasmic tail of gp41 contributes to resistance to antibody-mediated neutralization. Although non-human primate models of SIV infection are commonly used to estimate vaccine efficacy, the lack of broadly neutralizing MAbs has hampered development of antibody-based vaccine candidates in an SIV-macaque model. The broadly neutralizing MAb B404, which neutralizes multiple, diverse SIV isolates (Kuwata et al., 2013), is a useful tool for understanding the mechanism of neutralization in an SIV-macaque model and will contribute to the development of HIV-1 vaccines.

ACKNOWLEDGMENTS

We thank Dr. Hirofumi Akari for providing HSC-F cells. TZM-bl cells were obtained from Dr. John C. Kappes, Dr. Xiaoyun Wu, and Tranzyme Inc. through the NIH AIDS Research and Reference Reagent Program, Division of AIDS, NIAID, NIH. This work

was supported by MEXT KAKENHI Grant Number 10839786, the Program of Founding Research Centres for Emerging and Re-emerging Infectious Diseases, the Global COE program Global Education and Research Centre Aiming at the Control of AIDS and a grant-in-aid for scientific research (C-24591484) from the Ministry of Education, Culture, Sport, Science and Technology, Japan and a grant from the Ministry of Health, Welfare and Labour of Japan (H24-AIDS-007).

REFERENCES

Akari, H., Nam, K. H., Mori, K., Otani, I., Shibata, H., Adachi, A., et al. (1999). Effects of SIVmac infection on peripheral blood CD4+CD8+ T lymphocytes in cynomolgus macaques. *Clin. Immunol.* 91, 321–329.

Berlioz-Torrent, C., Shacklett, B. L., Erdtmann, L., Delamarre, L., Bouchaert, I., Sonigo, P., et al. (1999). Interactions of the cytoplasmic domains of human and simian retroviral transmembrane proteins with components of the clathrin adaptor complexes modulate intracellular and cell surface expression of envelope glycoproteins. *J. Virol.* 73, 1350–1361.

Bonavia, A., Bullock, B. T., Gisselman, K. M., Margulies, B. J., and Clements, J. E. (2005). A single amino acid change and truncated TM are sufficient for simian immunodeficiency virus to enter cells using CCR5 in a CD4-independent pathway. *Virology* 341, 12–23.

Derdeyn, C. A., Decker, J. M., Sfakianos, J. N., Wu, X., O'Brien, W. A., Ratner, L., et al. (2000). Sensitivity of human immunodeficiency virus type 1 to the fusion inhibitor T-20 is modulated by coreceptor specificity defined by the V3 loop of gp120. *J. Virol.* 74, 8358–8367.

DuBridge, R. B., Tang, P., Hsia, H. C., Leong, P. M., Miller, J. H., and Calos, M. P. (1987). Analysis of mutation in human cells by using an Epstein–Barr virus shuttle system. *Mol. Cell. Biol.* 7, 379–387.

Hatada, M., Yoshimura, K., Harada, S., Kawanami, Y., Shibata, J., and Matsushita, S. (2010). Human immunodeficiency virus type 1 evasion of a neutralizing anti-V3 antibody involves acquisition of a potential glycosylation site in V2. *J. Gen. Virol.* 91, 1335–1345.

Haynes, B. F., Gilbert, P. B., Mcelrath, M. J., Zolla-Pazner, S., Tomaras, G. D., Alam, S. M., et al. (2012). Immune-correlates analysis of an HIV-1 vaccine efficacy trial. *N. Engl. J. Med.* 366, 1275–1286.

Hirsch, V. M., Edmondson, P., Murphey-Corb, M., Arbeille, B., Johnson, P. R., and Mullins, J. I. (1989). SIV adaptation to human cells. *Nature* 341, 573–574.

Kodama, T., Wooley, D. P., Naidu, Y. M., Kestler, H. W. III, Daniel, M. D., Li, Y., et al. (1989). Significance of premature stop codons in env of simian immunodeficiency virus. *J. Virol.* 63, 4709–4714.

Kuwata, T., Katsumata, Y., Takaki, K., Miura, T., and Igarashi, T. (2011). Isolation of potent neutralizing monoclonal antibodies from an SIV-Infected rhesus macaque by phage display. *AIDS Res. Hum. Retroviruses* 27, 487–500.

Kuwata, T., Takaki, K., Yoshimura, K., Enomoto, I., Wu, F., Ourmanov, I., et al. (2013). Conformational epitope consisting of the V3 and V4 loops as a target for potent and broad neutralization of simian immunodeficiency viruses. *J. Virol.* 87, 5424–5436.

Kwong, P. D., and Mascola, J. R. (2012). Human antibodies that neutralize HIV-1: identification, structures, and B cell ontogenies. *Immunity* 37, 412–425.

LaBranche, C. C., Sauter, M. M., Haggarty, B. S., Vance, P. J., Romano, J., Hart, T. K., et al. (1995). A single amino acid change in the cytoplasmic domain of the simian immunodeficiency virus transmembrane molecule increases envelope glycoprotein expression on infected cells. *J. Virol.* 69, 5217–5227.

Lusso, P., Cocchi, F., Balotta, C., Markham, P. D., Louie, A., Farci, P., et al. (1995). Growth of macrophage-tropic and primary human immunodeficiency virus type 1 (HIV-1) isolates in a unique CD4+ T-cell clone (PM1): failure to downregulate CD4 and to interfere with cell-line-tropic HIV-1. *J. Virol.* 69, 3712–3720.

Manrique, J. M., Celma, C. C., Affranchino, J. L., Hunter, E., and Gonzalez, S. A. (2001). Small variations in the length of the cytoplasmic domain of the simian immunodeficiency virus transmembrane protein drastically affect envelope incorporation and virus entry. *AIDS Res. Hum. Retroviruses* 17, 1615–1624.

Matsumi, S., Matsushita, S., Yoshimura, K., Javaherian, K., and Takatsuki, K. (1995). Neutralizing monoclonal antibody against a external envelope glycoprotein (gp110) of SIVmac251. *AIDS Res. Hum. Retroviruses* 11, 501–508.

Mori, K., Ringler, D. J., Kodama, T., and Desrosiers, R. C. (1992). Complex determinants of macrophage tropism in env of simian immunodeficiency virus. *J. Virol.* 66, 2067–2075.

Platt, E. J., Wehrly, K., Kuhmann, S. E., Chesebro, B., and Kabat, D. (1998). Effects of CCR5 and CD4 cell surface concentrations on infections by macrophagetropic isolates of human immunodeficiency virus type 1. *J. Virol.* 72, 2855–2864.

Postler, T. S., and Desrosiers, R. C. (2013). The tale of the long tail: the cytoplasmic domain of HIV-1 gp41. *J. Virol.* 87, 2–15.

Reed, L. J., and Muench, H. (1938). A simple method of estimating fifty per cent endpoints. *Am. J. Epidemiol.* 27, 493–497.

Rerks-Ngarm, S., Pitisuttithum, P., Nitayaphan, S., Kaewkungwal, J., Chiu, J., Paris, R., et al. (2009). Vaccination with ALVAC and AIDSVAX to prevent HIV-1 infection in Thailand. *N. Engl. J. Med.* 361, 2209–2220.

Takeuchi, Y., Mcclure, M. O., and Pizzato, M. (2008). Identification of gammaretroviruses constitutively released from cell lines used for human immunodeficiency virus research. *J. Virol.* 82, 12585–12588.

Tamura, K., Peterson, D., Peterson, N., Stecher, G., Nei, M., and Kumar, S. (2011). MEGA5: molecular evolutionary genetics analysis using maximum likelihood, evolutionary distance, and maximum parsimony methods. *Mol. Biol. Evol.* 28, 2731–2739.

Vzorov, A. N., Gernert, K. M., and Compans, R. W. (2005). Multiple domains of the SIV Env protein determine virus replication efficiency and neutralization sensitivity. *Virology* 332, 89–101.

Vzorov, A. N., Weidmann, A., Kozyr, N. L., Khaoustov, V., Yoffe, B., and Compans, R. W. (2007). Role of the long cytoplasmic domain of the SIV Env glycoprotein in early and late stages of infection. *Retrovirology* 4, 94.

Wei, X., Decker, J. M., Liu, H., Zhang, Z., Arani, R. B., Kilby, J. M., et al. (2002). Emergence of resistant human immunodeficiency virus type 1 in patients receiving fusion inhibitor (T-20) monotherapy. *Antimicrob. Agents Chemother.* 46, 1896–1905.

Yoshimura, K., Shibata, J., Kimura, T., Honda, A., Maeda, Y., Koito, A., et al. (2006). Resistance profile of a neutralizing anti-HIV monoclonal antibody, KD-247, that shows favourable synergism with anti-CCR5 inhibitors. *AIDS* 20, 2065–2073.

Yusa, K., Maeda, Y., Fujioka, A., Monde, K., and Harada, S. (2005). Isolation of TAK-779-resistant HIV-1 from an R5 HIV-1 GP120 V3 loop library. *J. Biol. Chem.* 280, 30083–30090.

Yuste, E., Johnson, W., Pavlakis, G. N., and Desrosiers, R. C. (2005). Virion envelope content, infectivity, and neutralization sensitivity of simian immunodeficiency virus. *J. Virol.* 79, 12455–12463.

Yuste, E., Reeves, J. D., Doms, R. W., and Desrosiers, R. C. (2004). Modulation of Env content in virions of simian immunodeficiency virus: correlation with cell surface expression and virion infectivity. *J. Virol.* 78, 6775–6785.

Zhu, P., Chertova, E., Bess, J., Lifson, J. D., Arthur, L. O., Liu, J., et al. (2003). Electron tomography analysis of envelope glycoprotein trimers on HIV and simian immunodeficiency virus virions. *Proc. Natl. Acad. Sci. U.S.A.* 100, 15812–15817.

Zhu, P., Liu, J., Bess, J., Chertova, E., Lifson, J. D., Grisé, H., et al. (2006). Distribution and three-dimensional structure of AIDS virus envelope spikes. *Nature* 441, 847–852.

Conflict of Interest Statement: The authors declare that the research was conducted in the absence of any commercial or financial relationships that could be construed as a potential conflict of interest.

Received: 22 March 2013; accepted: 25 April 2013; published online: 14 May 2013.

Citation: Kuwata T, Takaki K, Enomoto I, Yoshimura K and Matsushita S (2013) Increased infectivity in human cells and resistance to antibody-mediated neutralization by truncation of the SIV gp41 cytoplasmic tail. Front. Microbiol. 4:117. doi: 10.3389/fmicb.2013.00117

This article was submitted to Frontiers in Virology, a specialty of Frontiers in Microbiology.

Journal of General Virology (2013), 94, 2710–2716 DOI 10.1099/vir.0.055590-0

Short Communication

Generation of a replication-competent simian–human immunodeficiency virus, the neutralization sensitivity of which can be enhanced in the presence of a small-molecule CD4 mimic

Hiroyuki Otsuki,[1] Takayuki Hishiki,[1] Tomoyuki Miura,[1] Chie Hashimoto,[2] Tetsuo Narumi,[2] Hirokazu Tamamura,[2] Kazuhisa Yoshimura,[3] Shuzo Matsushita[4] and Tatsuhiko Igarashi[1]

[1]Laboratory of Primate Model, Experimental Research Center for Infectious Diseases, Institute for Virus Research, Kyoto University, Kyoto 606-8507, Japan

[2]Department of Medicinal Chemistry, Institute of Biomaterials and Bioengineering, Tokyo Medical and Dental University, Tokyo 101-0062, Japan

[3]AIDS Research Center, National Institute of Infectious Diseases, Tokyo 162-8640, Japan

[4]Division of Clinical Retrovirology and Infectious Diseases, Center for AIDS Research, Kumamoto University, Kumamoto 860-0811, Japan

Correspondence
Tatsuhiko Igarashi
tigarash@virus.kyoto-u.ac.jp

Received 29 May 2013
Accepted 10 September 2013

Simian–human immunodeficiency virus (SHIV) carrying the envelope from the clade B clinical human immunodeficiency virus type 1 (HIV-1) isolate MNA, designated SHIV MNA, was generated through intracellular homologous recombination. SHIV MNA inherited biological properties from the parental HIV-1, including CCR5 co-receptor preference, resistance to neutralization by the anti-V3 loop mAb KD-247 and loss of resistance in the presence of the CD4-mimic small-molecule YYA-021. SHIV MNA showed productive replication in rhesus macaque PBMCs. Experimental infection of a rhesus macaque with SHIV MNA caused a transient but high titre of plasma viral RNA and a moderate antibody response. Immunoglobulin in the plasma at 24 weeks post-infection was capable of neutralizing SHIV MNA in the presence but not in the absence of YYA-021. SHIV MNA could serve a model for development of novel therapeutic interventions based on CD4-mimic-mediated conversion of envelope protein susceptible to antibody neutralization.

Control of primate lentiviral infection by antibodies directed against viral envelope protein is theoretically feasible. This was confirmed by the successful protection of macaque monkeys from challenge inoculation with simian–human immunodeficiency virus (SHIV) carrying an envelope protein (Env). Env was derived from a laboratory strain of human immunodeficiency virus type 1 (HIV-1) through the passive immunization of neutralizing mAbs directed against HIV-1 (Mascola *et al.*, 2000; Nishimura *et al.*, 2003). This neutralization is consistent with the results normally seen in cell culture systems.

In contrast, clinical isolates of HIV-1 that have not been subjected to extensive passage in T-cell lines are generally resistant to antibody-mediated neutralization (Moore *et al.*, 1995). It has been shown that virus in infected individuals is under selective pressure to develop a variety of means to evade attack by neutralizing antibodies, including sequence variation, glycosylation, tertiary structural shielding formed by the Env trimer and the rapid kinetics of conformational changes of Env, which affect fusion between the viral envelope and the plasma membrane of target cells (Kong & Sattentau, 2012). Although four major neutralizing epitopes have been identified in HIV-1 Env (i.e. the V1/V2 loop, the glycan-V3 site and CD4-binding site of gp120, and the membrane-proximal external region of gp41), for reasons that are as yet unclear few reports of antibodies directed against these epitopes capable of neutralizing a broad range of isolates have been published (Kwong & Mascola, 2012). High titres of antibodies directed against the V3 loop are elicited in individuals during the early phase of HIV-1 infection, but these are incapable of neutralizing the virus because the epitope in functional Env trimer is probably shielded from the antibody (Davis *et al.*, 2009b). Therefore, it is necessary to develop a means of rendering these epitopes accessible to

One supplementary table and five supplementary figures are available with the online version of this paper.

the antibodies, to make antibody-mediated suppression of HIV-1 a valid therapeutic option.

It has been reported that neutralization mediated by antibodies directed against the V3 loop (Lusso *et al.*, 2005) or CD4-induced epitope (CD4i) (Thali *et al.*, 1993) can be enhanced in the presence of soluble CD4 (sCD4). It is known that the interaction of Env with sCD4 drives a conformational change of the viral protein and makes the cryptic/occult epitopes accessible to these antibodies (Wyatt *et al.*, 1998). Small molecules that emulate sCD4 for its interaction and subsequent induction of conformational change of Env may be employed to intensify antibody-mediated interventions against HIV-1 infection. Compounds with the above-mentioned properties (i.e. NBD-556 and NBD-557) have been reported previously (Zhao *et al.*, 2005). NBD-556 has been shown in cell culture to interact with the CD4-binding pocket to induce a conformational change in gp120 (Madani *et al.*, 2008) and enhance exposure of the Env of primary HIV-1 isolates to neutralizing epitopes (Yoshimura *et al.*, 2010).

The present study was performed to evaluate small-molecule CD4-mimic-based enhancement of antibody-mediated virus neutralization, in the context of virus infection *in vivo*. The SHIV/macaque monkey model of AIDS is particularly suitable for such studies, as SHIV carries the HIV-1 Env and the neutralization sensitivity of SHIV is comparable to that of the parental HIV-1 (Shibata & Adachi, 1992).

As NBD-556, unlike sCD4, inhibits infection with select HIV-1 isolates (Yoshimura *et al.*, 2010), we generated a new SHIV strain carrying Env, the sensitivity of which to antibody-mediated neutralization is enhanced in the presence of a CD4 mimic. An HIV-1 isolate (MNA), previously designated primary isolate HIV-1 Pt.3, was used as the source of Env, as the viral protein has been reported to interact with NBD-556 (Yoshimura *et al.*, 2010). While the virus belongs to a distinct subset of HIV-1 isolates, as mentioned above, it has also been reported to utilize the CCR5 molecule to gain entry into target cells, a property that is shared by the majority of HIV-1 strains (Yoshimura *et al.*, 2010). A mAb directed against the tip of the V3 loop (GPGR motif), KD-247 (Eda *et al.*, 2006), was employed to assess this concept, as HIV-1 MNA is resistant to KD-247-mediated neutralization, despite carrying the exact epitope sequence in the tip of the V3 loop, and is converted to being sensitive to the antibody by NBD-556 in a dose-dependent manner (Yoshimura *et al.*, 2010).

First, we reproduced the results of Yoshimura *et al.* (2010) using a neutralization assay employing TZM-bl cells (Platt *et al.*, 1998), obtained from the National Institutes of Health (NIH) AIDS Reagent Program (Fig. S1, available in JGV Online). The virus was resistant to KD-247, as described previously, and required almost 50 μg ml^{-1} of the antibody to achieve 50 % neutralization in our assay. However, the observed resistance was eliminated in the presence of 2 μM NBD-556; 50 % neutralization was achieved in the presence of ~0.1 μg KD-247 ml^{-1}, corresponding to 1/500 of the amount of the antibody to achieve the same degree of neutralization in the absence of the CD4 mimic.

With reproduction of the properties of HIV-1 MNA Env, we generated an SHIV strain carrying Env through intracellular homologous recombination, as described previously (Fujita *et al.*, 2013) with minor modifications (Fig. S2). DNA fragments representing the 5′ and 3′ ends of the SHIV genome (fragments I and II, respectively) were amplified by PCR from the proviral DNA plasmid SHIV KS661. A DNA fragment containing *env* (fragment III) was amplified from cDNA of the HIV-1 MNA genome, which was prepared from virus particles (virion-associated RNA) in the culture supernatant of PM1/CCR5 cells (Yusa *et al.*, 2005) infected with the virus. The PCR primers used are listed in Table S1. Using a FuGENE HD transfection reagent, lipofection was performed on the C8166-CCR5 cells (Shimizu *et al.*, 2006) to co-transfect them with 0.2 μg DNA. A cytopathic effect, presumably caused by the emerged recombinant virus, was observed on day 13 post-transfection. The emerged virus, designated SHIV MNA, carried the entire gp120 and three-quarters of gp41 from HIV-1 MNA Env (Fig. 1a). The rest of Env was from SHIV KS661, the Env of which was derived from HIV-1 89.6 (Shinohara *et al.*, 1999). The CD4 binding site, and the regions and elements that reportedly interact with NBD-556 (Madani *et al.*, 2008; Yoshimura *et al.*, 2010), are preserved in SHIV MNA Env (Fig. S3). The virus was replication competent in PM1/CCR5 cells (data not shown).

As HIV-1 MNA has been suggested to be a CCR5-utilizing virus, we were intrigued as to whether SHIV MNA inherited the trait from the parental virus. We subjected SHIV MNA and the parental HIV-1 MNA to a co-receptor usage assay as described previously (Nishimura *et al.*, 2010), with minor modifications (Fig. S4). As expected, SHIV MNA was shown to utilize CCR5 as an entry co-receptor.

We next assessed the neutralization profiles of SHIV MNA in comparison with the parental HIV-1 MNA, as described previously (Li *et al.*, 2005; Wei *et al.*, 2002). Both SHIV MNA and HIV-1 MNA showed essentially no neutralization by KD-247 up to 25 μg ml^{-1}, and 50 % neutralization was achieved at 50 μg ml^{-1} (Fig. 1b). As the CD4 mimic, we employed YYA-021, a compound generated and characterized through studies concerning the structure–activity relationships of small molecules (Narumi *et al.*, 2010, 2011, 2013; Yamada *et al.*, 2010). The compound was shown to be slightly less potent but to exhibit substantially lower toxicity than NBD-556, and was therefore a suitable choice for our purposes in future studies in animal models. SHIV MNA was resistant to neutralization by YYA-021 at all concentrations examined, except 25 and 50 μM, and showed a neutralization profile almost identical to that of HIV-1 MNA (Fig. 1c). To further characterize the

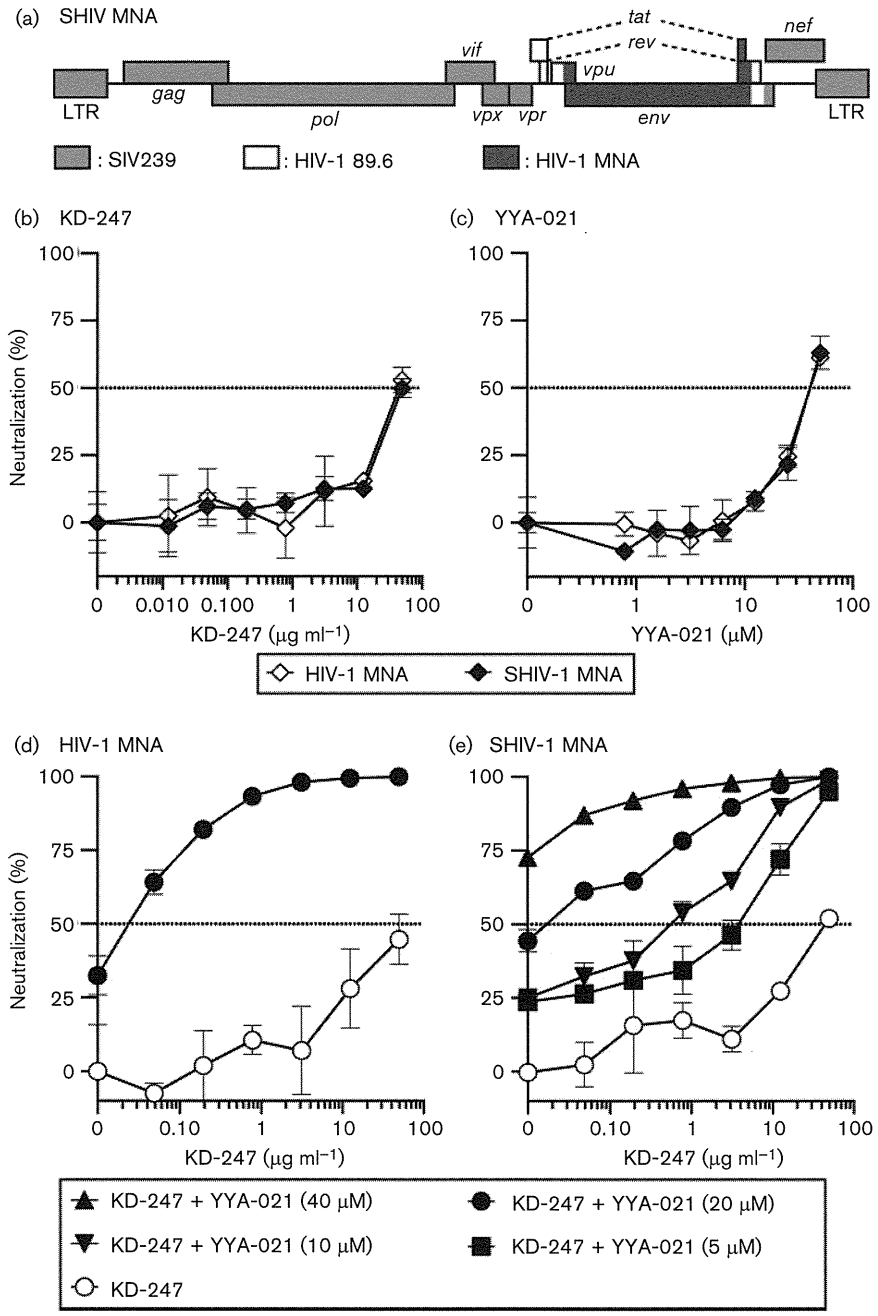

Fig. 1. Genomic organization (a) and neutralization sensitivity (b–e) of SHIV MNA. (a) Grey shaded boxes represent genes derived from SIV239, open boxes those from HIV-1 89.6 and dark grey shaded boxes those from HIV-1 MNA. LTR, long terminal repeat. (b–e) Percentage neutralization was calculated as 100×[1−(RLU.N−RLU.B)/(RLU.V−RLU.B)], where RLU is relative luciferase units; RLU.N is RLU in wells with cells, virus and KD-247 and/or YYA-021; RLU.V is RLU in wells with cells and virus; and RLU.B is RLU in wells with cells.

biological properties of SHIV MNA Env, a set of entry assays was conducted (Fig. S5). The *env* genes cloned from SHIV MNA and HIV-1 MNA were utilized to generate pseudotyped viruses. These pseudotypes were inoculated into TZM-bl cells in the presence of increasing amounts of NBD-556, YYA-021 or sCD4. A control group was derived from another virus preparation pseudotyped with amphotropic murine leukemia virus (A-MLV) Env (Landau *et al.*, 1991). When the efficiency of entry was defined by intracellular luciferase activities, virtually no difference was observed between Envs of SHIV MNA and the parental HIV-1. Thus, SHIV MNA Env replicated in